Nutrient limitations regulate soil greenhouse gas fluxes from tropical forests: evidence from an ecosystem-scale nutrient manipulation experiment in Uganda

5   Joseph Tamale[1,5], Roman Hüppi[4], Marco Griepentrog[3], Laban Frank Turyagyenda[5], Matti Barthel[4], Sebastian Doetterl[3], Peter Fiener[1*], and Oliver van Straaten[2,6]

[1]Institute of Geography, University of Augsburg, Augsburg, 86159, Germany
[2]Environmental Control Department, Northwest German Forest Research Institute, 37079, Germany
10   [3]Soil Resources, Department of Environmental Systems Science, ETH, Zurich, 8092, Switzerland
[4]Sustainable Agroecosystems, Department of Environmental Systems Science, ETH, Zurich, 8092, Switzerland
[5]Ngetta Zonal Agricultural Research and Development Institute (NGEZARDI), P. O. Box 52, Lira, Uganda
[6]Soil Science of Tropical and Subtropical Ecosystems, Büsgen-Institute, University of Göttingen, Göttingen, 37077, Germany

*Correspondence to: Peter Fiener (peter.fiener@geo.uni-augsburg.de)

Abstract. Soil macronutrient availability is one of the abiotic controls that alters the exchange of greenhouse gases (GHGs) between the soil and atmosphere in tropical forests. However, evidence on macronutrient regulation of soil
20   GHG fluxes from central African tropical forests is still rare—limiting our understanding of how these biomes could respond to potential future increases in N and P deposition. The aim of this study was to disentangle the regulation effect of soil nutrients on soil GHG fluxes from a Ugandan tropical forest reserve in the context of increasing N and P deposition. Therefore, a large-scale nutrient manipulation experiment (NME) based on 40 m x 40 m plots with different nutrient addition treatments (nitrogen (N), phosphorus (P), N + P, and control) was established in Budongo Forest
25   Reserve. Soil CO_2, CH_4, and N_2O fluxes were measured monthly using permanently installed static chambers for 14 months. Total soil CO_2 fluxes were partitioned into autotrophic and heterotrophic components through a root trenching treatment. In addition, soil temperature, soil water content, and nitrates were measured in parallel to GHG fluxes. N addition (N, N + P) resulted in significantly higher N_2O fluxes in the transitory phase (0-28 days after fertilization, *p < 0.01*), because N fertilization likely increased soil N beyond the microbial immobilization and plant nutritional
30   demands leaving the excess to be nitrified or denitrified. Prolonged N fertilization however, did not elicit a significant response in background (measured more than 28 days after fertilization) N_2O fluxes. P fertilization marginally and significantly increased transitory (*p = 0.05*) and background (*p = 0.01*) CH_4 consumption, probably because it enhanced methanotrophic activity. Addition of N and P together (N + P) resulted in larger CO_2 fluxes in the transitory phase (*p = 0.01*), suggesting a possible co-limitation of both N and P on soil respiration. Heterotrophic (microbial)
35   CO_2 effluxes were significantly higher than the autotrophic (root) CO_2 effluxes (*p < 0.01*) across all treatment plots with microbes contributing about two thirds of the total soil CO_2 effluxes. However, neither heterotrophic nor autotrophic respiration significantly differed between treatments. The results from this study suggest that the feedback of tropical forests to the global soil GHG budget could be disproportionately altered by increases in N and P availability over these biomes.

1 Introduction

Tropical forest soils play an important role in the earth's radiative balance by sequestering and releasing significant amounts of carbon dioxide (CO_2), methane (CH_4), and nitrous oxide (N_2O) (Mosier et al., 2004). It is estimated that tropical forest soils emit about 1.3 ± 0.3 Tg N_2O yr^{-1} (Butterbach-Bahl et al., 2004), capture 6.4 Tg CH_4 yr^{-1} (Dutaur and Verchot, 2007), and sequester about 10 % of the total atmospheric CO_2 via photosynthesis; and account for about 30 % of the world's soil C stocks (Jobbágy and Jackson, 2000; Malhi and Phillips, 2004).

The rate and magnitude of the specific plant- and soil microbial-processes that produce (CO_2: autotrophic and heterotrophic respiration, N_2O: denitrification and nitrification, CH_4: enteric fermentation and methanogenesis) and consume (CO_2: photosynthesis, CH_4: oxidation) greenhouse gases (GHGs) in and at the soil-atmospheric interface are constrained by a multiplicity of biotic and abiotic controls (Mosier et al., 2004). These controls include vegetation communities (Veber et al., 2018), soil moisture (Sjögersten et al., 2018), soil temperature (Holland et al., 2000), geochemistry (given its control on microbial abundance (Gray et al., 2014) and soil organic carbon stabilization (Doetterl et al., 2015)), as well as macronutrient availability (especially N and P) (Oertel et al., 2016).

Macronutrient replenishment in undisturbed tropical forests is inherently via litter input (for both N and P, (Tanner et al., 1998)) and rock weathering (for P, (Hedin et al., 2003)) processes. However, the past three decades have seen an increase in the levels of N and P deposition over most tropical regions (including central Africa) due to widespread deforestation and biomass burning (Bauters et al., 2019; Galloway et al., 2004). Currently, the central African region receives about 18.5 kg N ha^{-1} (Bauters et al., 2019) and $1.8 – 2.5$ kg P ha^{-1} (Tamatamah et al., 2005) each year due to high fire-derived N deposition (Bauters et al., 2019) and P rich biomass aerosols (Barkley et al., 2019), respectively. Increased anthropogenic N and P deposition over tropical forest biomes disrupts ecosystem stoichiometric equilibrium thereby affecting biogeochemical cycling of N and P (Bauters et al., 2019), as well as, the exchange of GHGs between the soil and atmosphere (Corre et al., 2014). One way of understanding how increases in N and P availability (for instance through deposition) affect soil GHG fluxes from tropical forests is through large scale nutrient manipulation experiments (NMEs). NMEs purposely use large doses of N and P (e.g. Cleveland and Townsend, 2006 (150 kg N ha^{-1} yr^{-1} and 150 kg P ha^{-1} yr^{-1}), Hall and Matson, 2003 (100 kg N ha^{-1} yr^{-1} and 40 kg P ha^{-1} yr^{-1})) to simulate how future nutrient enrichment of tropical forests (through deposition) could affect soil GHG fluxes (among other ecosystem processes) (Corre et al., 2010).

To date, several NMEs have been carried out across the tropics (e.g. Corre et al., 2010; Wei et al., 2008), and the outcome has been a consensus that addition of N to an already N-rich tropical forest ecosystem results in increased N_2O emissions (Corre et al., 2014; Martinson et al., 2013; Zhang et al., 2008). For N-rich forest ecosystems, an increase in available soil N beyond the microbial immobilization and plant nutritional demands, results in the excess being nitrified or (and) denitrified by soil microbes (Corre et al., 2014). However, several studies suggest that increased availability of N not only reduces fine root biomass but also curtails microbial activity leading to reduced autotrophic (Cusack et al., 2011) and heterotrophic respiration (Chen et al., 2010; DeForest et al., 2006; Koehler et al., 2009a), respectively. Notably, there are varying results on how N addition affects CH_4 uptake from tropical forest soils. For instance, Veldkamp et al. (2013) found no effect of N on CH_4 uptake while Du et al. (2019) measured reduced CH_4 consumption following addition of N to a tropical forest, with the latter study suggesting an inhibitory effect of N on CH_4 uptake (Bodelier and Steenbergh, 2014; Seghers et al., 2003; Zhang et al., 2011). Aronson and Helliker (2010)

argue that the observed differences in the measured CH_4 fluxes in the two separate studies were likely due to the different amounts of N added in the respective experimental setups. They argued that low amounts of N stimulate CH_4 uptake while high amounts inhibit it.

With respect to P, it has been shown that P availability opens up the N cycle by stimulating soil organic matter mineralization, releasing excess N for soil nitrification or (both) denitrification processes (Mori et al., 2010). It is also urged that P availability has a positive effect on both autotrophic and heterotrophic components of soil respiration (Mori et al., 2013). P not only stimulates fine root growth (Chen et al., 2010) but also regulates organic matter decomposition (Mori et al., 2018). However, studies elucidating P limitation of organic matter decomposition in the P deficient tropics remain rare and even the few available studies on the regulation effect of P on leaf litter mass loss rates are inconclusive (Cleveland and Townsend, 2006). This might explain why contrasting results were reported from two similar experiments carried out on P depleted soils in Hawaii (Hobbie and Vitousek, 2000) and the Brazilian Amazon (McGroddy et al., 2008). Hobbie and Vitousek (2000) reported an increase in litter mass loss rate while McGroddy et al. (2008) did not detect any change, suggesting that the relationship between P availability and organic matter decomposition is complex (Cleveland and Townsend, 2006). Similarly, literature on the interaction between N and P in regulating CH_4 fluxes from tropical forests remains limited.

Despite the recognition that N and P affect soil GHG fluxes and the fact that tropical forest ecosystems could subtly respond to potential future increases in N and P deposition (Bobbink et al., 2010; Li et al., 2006), the magnitude and direction of this response remains unclear for African tropical forests. To date, only a handful of nutrient manipulation experiments (NMEs) focusing on tropical forests response to shifts in ecosystem N and P dynamics have been carried out. Of these studies, just a few included both N and P treatments in their experimental setups (e.g. Corre et al., 2014). Yet, P deficiency typical of tropical soils can have direct impacts on ecosystem biomass production if the limitation is lifted (John et al., 2007). Furthermore, nearly all the studies conducted in (sub-) tropical forest ecosystems were so far concentrated in China (Jiang et al., 2016; Yan et al., 2008; Zheng et al., 2016), Central America (Corre et al., 2014; Koehler et al., 2009a; Matson et al., 2014) and South America (Martinson et al., 2013; Müller et al., 2015; Wolf et al., 2011).

Unfortunately, no single controlled experiment has simulated the effects of elevated soil nutrient inputs on soil greenhouse gas fluxes from African tropical forests despite the projected increase in N and P deposition over theses biomes (Galloway et al., 2004) and the fact that they represent a significant proportion of global tropical forests (27 % ; Saachi et al., 2011). It was for this reason that a replicated completely randomized NME was established in a Ugandan tropical forest reserve to investigate the role nitrogen and phosphorus have in regulating soil GHG fluxes in the context of changing N and P deposition rates over the tropics. It was hypothesized that:

1) addition of N or N + P to a tropical forest ecosystem would result in increased N_2O emissions coming from excess availability of bio-available N beyond microbial immobilization and plant N demands, decreased CH_4 uptake due to negative effects of N addition on soil methanotrophs, and reduced CO_2 effluxes largely attributed to reduction in both root and microbial respiration upon addition of N;

2) adding P to a tropical forest ecosystem would stimulate release of N from soil organic matter and consequently lead to increased N_2O emissions, higher CO_2 effluxes linked to increased root activity and decomposition of soil organic matter, and increased CH_4 uptake due to stimulation of methanotrophic activity.

2 Materials and Methods

2.1 Study site description

The study was conducted in Budongo Forest Reserve, a semi-deciduous tropical forest, located in the northwestern part of Uganda (1°44'28.4" N, 31°32'11.0" E). The forest reserve spans over 825 km^2 and is extensively diverse in respect to forest communities, with *Cynometra alexandria, Chryophyllum albidum, Meosopsis eminii and Diospyros abyssinica* as the dominant tree species (Eggeling, 1947). The long-term mean annual temperature and precipitation over the study area is 25 °C and 1700 mm, respectively (Lukwago et al., 2020). Rainfall is distributed into two rainy seasons (i.e. March to May and August to November) punctuated by a strong dry season (December to February), and a weak dry season (June to July) (Lukwago et al., 2020). It is worth noting that the amount of rainfall received during the field campaign (2385 mm, Fig. 2d) was higher than the long-term mean annual precipitation for this region. The weather data for the experiment period was obtained from a climatic station installed at Budongo Conservation Field station (2 km northwest of the study site), and was beneficial to understand how precipitation constrained soil greenhouse gas fluxes given its direct control on water filled pore space. The soils at the experimental site are highly weathered—classified as Lixisols (IUSS Working Group WRB, 2014), and are developed on a Precambrian gneissic-granulitic basement complex (van Straaten, 1976).

2.2 Experimental design

The study was conducted within the framework of a running nutrient manipulation experiment (NME). The NME study used a completely randomized design to investigate how the three macronutrients (applied individually as nitrogen (N), phosphorus (P), and potassium (K) and in all possible combinations (N+ P, N+ K, P + K, N+ P + K) as treatments) constrained key ecosystem processes (particularly nutrient cycling, and net primary productivity) in comparison to the unamended control. Each of the eight treatments was replicated four times (hence, n = 32 plots; 8 treatments x 4 replications). While the NME included a K treatment, the soil GHG flux study—the basis for this manuscript was conducted on the N, P and N + P (combination of N and P) plots, and compared to the untreated control plots (n = 16). Only N and P (among nutrient addition plots) were exclusively considered for soil GHG flux measurements because their availability has been shown to limit soil greenhouse gas fluxes from tropical forest biomes. Each treatment plot measured 40 m x 40 m in size but measurements were conducted in the inner measurement core (30 m x 30 m) to avoid boundary effects. A spacing of at least 40 m between experimental plots was ensured to prevent spillover of applied nutrients from the neighboring plots. In order to elicit an ecosystem response, N was applied at a rate of 125 kg N ha^{-1} yr^{-1} in form of urea $((NH_2)_2CO)$, and P at 50 kg P ha^{-1} yr^{-1} as triple superphosphate $(Ca(H_2PO_4)_2)$. The types of fertilizers and application rates used in this study were identical to those used in the Wright et al. (2011) NME. The fertilizer was applied by hand, and in four split dozes every year. Specifically, 31.3 kg N ha^{-1} and 12.5 kg P ha^{-1} were applied to the plots of the NME every three months between May 2018 and June 2020.

2.3   Baseline soil physico-biochemical characterization

Prior to the first fertilizer application, soil samples were taken in all the treatment plots for baseline soil physico-biochemical analysis. These included; texture, bulk density, soil pH, total soil organic carbon (TOC) stocks, total nitrogen stocks, C/N ratio, exchangeable bases, ECEC, and Bray extractable P. For the 0-10 cm depth, soil monoliths (20 cm (L) x 20 cm (W) x 10 cm (D)) were carefully taken from ten different locations within each plot of the NME (n = 32 plots) using a spade. However, for deeper soil layers (0-30 cm and 30- 50 cm), samples were obtained outside the established NME plots in order to minimize modifications to the microenvironment inside the NME plots. Deeper soil sampling was done during a reconnaissance survey conducted at approximately 500 m from the current location of the NME site. During the reconnaissance survey, sixteen plots (n = 16) were established and samples taken from five different locations in each plot for every depth interval (i.e. 0-30 cm and 30- 50 cm) using an auger (diameter = 30 mm). The samples from each depth were mixed thoroughly in a basin, and about 500 g of the homogenized samples sent to the soils laboratory of the University of Göttingen, Germany, for analysis. Soil texture was determined using a Bouyoucos hydrometer. Soil pH was determined in 1:2.5 (soil water) suspension. Soil bulk density for every depth in each plot was calculated from the mass of oven dried soil (at 105°C for 48 hours) and the volume of the Kopecky ring (volume = 251 cm^3) used in collecting the soil sample. Note that soil bulk density was corrected for stone content. The soils were tested for presence of inorganic carbon (IC) using dilute hydrochloric acid, and were found to be devoid of any IC. Hence, TOC and N were determined using a CN elemental analyzer (Vario EL Cube, Elementar Analysis Systems GmbH, Hanau, Germany) and stocks later calculated from bulk density measurements. Exchangeable base cations (Ca, Mg, K, Na, Al, and ECEC) were determined on the 1-2 mm earth fraction of the collected soil samples.

2.4   Soil greenhouse gas fluxes and soil environmental control measurements

Soil CO_2, CH_4 and N_2O fluxes were measured monthly over a period of fourteen months (May 2019 to June 2020). In every replicate plot's inner measurement core, four chamber bases (fabricated from a 250 mm PN10 PVC pipe and each with an area = 0.044 m^2, and volume = about 12 L) were randomly installed at the soil surface, to a depth of about 0.03 m. Installation of chamber bases was done at the beginning of April 2019, a month prior to the GHG flux measurements, and chamber bases remained permanently in place for the entire measurement period. Litter was not removed from the chamber. However, all the chamber bases were always maintained vegetation free throughout the gas sampling period in order to avoid measuring plant night respiration during chamber closure. On the sampling day, chamber bases were covered with vented polyvinyl hoods fitted with sampling ports. A pooled gas sample was then obtained every 3, 13, 23, and 33 minutes using an airtight Luer Lock syringe following the pooling approach described in detail by Arias-Navarro et al. (2013). The 30 minute maximum chamber closure period used in this study was well under the threshold recommended by Pavelka et al. (2018)), but, comparable to other tropical GHG flux studies (e.g. Corre et al. (2010), Koehler et al. (2009a), Matson et al. (2017)). To check if the pooling worked correctly, both the pooled and un-pooled (an average of four individual chamber measurements) samples were taken for the month of February 2020 for analysis. Both methods produced very comparable results (Supplementary Fig. 1). Soil GHG fluxes were always measured between 9 am and 4 pm throughout the entire study period, while for each measurement day, the sequence of plots to be measured was randomly chosen. Together with the very low diurnal variability of air (0.6

± 0.04 °C; mean ± SE) and soil (0.2 ± 0.03 °C; mean ± SE) temperatures at this tropical forest site, time of measurement of individual gas chambers should, if at all, only have a minimal effect on the measured gas fluxes. All collected gas samples were stored in Labco Exetainers (Labco Limited, Lempeter, UK) with screw-on plastic caps fitted with Labco

190   Grey Chlorobutyl Septum because these exetainers have been demonstrated to remain airtight for periods spanning up to six months (Hassler et al., 2015). Additionally, all the plastic caps were screwed on to the exetainers by hand and "quarter turned" prior to sampling to ensure that they were airtight (Pavelka et al., 2018). All the gas-filled exetainers were shipped to the Department of Environmental Systems Science, ETH Zürich, Switzerland for analysis using a gas chromatograph (GC; Scion 456-GC Bruker, Germany) within a period of four months from sampling. The GC was

195   equipped with an electron capture detector (N_2O), flame ionization detector (CH_4), thermal conductivity detector (CO_2), and auto-sampler. GC concentrations of the individual gas species of interest (CO_2, CH_4 and N_2O) were then calculated by comparing the peak areas of the measured samples to the respective peak areas of a suite of standard gas samples. Next, flux rates of individual gases at the soil-atmospheric interface were calculated based on either linear increase or decrease in gas concentrations during chamber closure following Eq. 1 in Butterbach-Bahl et al. (2011).

200    $$GHG_{flux} = \frac{V_{ch} * GHG_m * S * 10^6 * 60}{A_{ch} * GHG_v * 10^9} \qquad (1)$$

where GHG_{flux} is given as a positive flux to the atmosphere and a negative flux into the soil [µg m^{-2} h^{-1}], V_{ch} is the chamber volume [m^3], GHG_m is the molar mass of the different gases [g mol^{-1}], S is the slope of a linear regression calculated based on the increase or decrease in gas concentrations during chamber closure [ppm min^{-1}], A_{ch} is the chamber ground area [m^2], GHG_v is the molar volume of the different gases [m^3 mol^{-1}]. Note that the constants 10^6,

205   10^9, and 60 were used to convert grams into micrograms, parts per million into cubic meters, and minutes into hours. GHG_v was adjusted to air temperature and pressure in the field using ideal gas law following Eq. 2:

$$GHG_v = 0.02241 * \frac{273.15 + T_f}{273.15} * \frac{P_f}{P_s} \qquad (2)$$

where T_f is the air temperature [°C] and P_f is the pressure [Pa] at the field site, while P_s is the pressure at sea level [Pa]. As a quality check, the linearity of CO_2 increase during chamber closure was inspected by comparing the CO_2

210   concentrations (of each chamber measurement) with time since chamber closure, and thereafter, determined the goodness of fit for the linear regression model (the R^2). The R^2 for all measurement was 0.992 ± 0.001 (mean ± SE). Additionally, the measured gas concentrations from the GC were checked against the standards and the GC's minimum detection limit to ensure that the changes in gas concentrations during chamber closure were well above its minimum detection limit.

215   In parallel to gas flux measurements, soil environmental controls particularly soil temperature, volumetric water content, and soil mineral nitrogen (ammonium (NH_4^+) and nitrate (NO_3^-)) were measured. Soil temperature and volumetric water content were determined at 0.05 m soil depth adjacent to each of the four-installed chamber bases per replicate plot. A digital thermometer (Greisinger GMH 3230, Germany) fitted with an insertion probe and a calibrated ML3 ThetaProbe soil moisture sensor (AT Delta-T Devices Limited, United Kingdom) were used to

220   determine soil temperature and soil volumetric water content, respectively. Soil mineral nitrogen was determined by obtaining a soil sample in a Kopercky ring at 0.05 m depth (from the soil surface) and 1 m distance from each of the installed chamber per replicate. The obtained soil samples (from each replicate plot) were pooled together and

thoroughly mixed. Next, 100 and 150 g of the pooled soil samples were extracted with 100 and 600 mL $CaCl_2$ solution for determination of NO_3^- and NH_4^+ concentrations respectively using the RQflex® 10 reflectometer. RQflex® 10 reflectometer is part of the reflectoquant system comprising of a reflectometer, batch-specific barcode and test strips. The test strips used in this study had a 3 - 90 and 0.2 - 7 mg L^{-1} detection range for nitrates (NO_3-N) and ammonium (NH_4-N), respectively.

To understand the contribution of autotrophic (root) and heterotrophic (microbial) sources to total soil respiration, a trenching treatment was done in all the plots following the protocol of Wang and Yang (2007). Prior to trenching, root biomass distribution with depth was determined in order to establish where most roots were located. Root biomass estimation involved digging three profile pits measuring 1 m (L) x 1 m (W) x 1.1 m (D) at the forest site. In every pit, ten soil monoliths (each measuring: 20 cm (L) x 20 cm (W)) were carefully cut out (using a spade and hoe) following a 10 cm depth interval from the surface down to 1 m. The soil monoliths were thoroughly washed to isolate the roots from the bulk soil. The root samples were oven dried at 60 °C for 48 hours and weighed to determine the root biomass per depth increment. The root biomass for each depth interval was calculated as the mean of the root biomass from the three pits for that interval. It was established that over 90 % of the roots were within the top 0.6 m of the soil profile. Therefore, a circular trench (about 0.60 m in diameter) was dug to a depth of about 0.6 m at the center of all the plots, thereby creating a soil mass free of roots. All the trenches were lined with a heavy-duty plastic sheet to prevent roots from growing back into the trenched soil mass. The trenched soil mass and the proximally neighboring un-trenched (reference) zone (about 1 m apart) were respectively installed with a chamber base. Both the trenched and reference chamber bases had a design (area = 0.044 m^2, and volume = about 12 L) identical to the one used in the NME soil GHG flux study. The installed chamber bases were left standing for six months, before the first measurements began in November 2019. This ensured that a large proportion of the cut roots in the trenched soil mass decomposed before the start of the CO_2 measurements. CO_2 measurements were conducted monthly for a period of 4 months (starting in November 2019 and ending in February 2020). The selected measurement time window represented the transition between the wet season and the long dry season, allowing us to capture how soil moisture constrained the different soil CO_2 efflux sources. After the completion of flux measurements, root coring was done to a depth of 0.30 m at two locations directly adjacent to both the trenched and un-trenched chambers, in order to determine if the trenching approach was effective in reducing the amount of living root biomass in the trenched zone. It was established that there was a 73 % and 63 % reduction in fine root biomass, and coarse root biomass, respectively, in the trenched zone in comparison to the reference zone. Heterotrophic (microbial) respiration was equal to the CO_2 effluxes from the trenched chamber while autotrophic (root) respiration was the difference between CO_2 effluxes from the reference and trenched chambers.

2.5   Statistical Analysis

Prior to statistical analysis, transitory N_2O fluxes from N addition plots (N, and N + P) were detrended to compensate for absence of frequent measurements immediately after fertilization coming from sampling GHGs monthly. Detrending involved using a log-normal fit between the measured N_2O fluxes and time since fertilization (until day 42), and this explained 43 % of the observed variability in the N_2O data during the transitory phase (*p < 0.05*). Additionally, GHG flux and soil environmental control data were aggregated based on seasons (wet and dry) and

phases (transitory; 0-28 days from the date of fertilization, and background; more than 28 days after fertilization). Furthermore, despite monitoring soil NO_3^- and NH_4^+ on a monthly basis throughout the measurement period, only the soil NO_3^- data set was used in the analysis because soil NH_4^+ was mostly low and often below the detection limit of the reflectometer at majority of the sampling time points.

265 Data was checked for normality and homogeneity of variance (homoscedasticity) across treatment groups, seasons, and phases before implementing parametric tests (i.e. linear mixed effects model (LMEMs), and one-way analysis of variance (ANOVA)). Normality of the respective data was inspected by use of diagnostic plots (histograms and quantile-quantile plots), and the Shapiro-Wilk normality test, while heteroscedasticity was determined with the Levene test and by inspecting residual plots of fitted values. In case of heteroscedasticity and non-normal distribution of the

270 data, either a logarithmic or a Tukey transformation was applied on the dataset. However, if normality of the data and homogeneity of variance were not restored by the transformations, an equivalent non-parametric statistical test was selected. The Spearman's correlation coefficient test was used to check the relationship between the measured background soil GHG fluxes and soil environmental controls.

To determine differences in mean soil GHG fluxes between treatments, one way ANOVA test was used with GHG

275 species and treatments included in the model as response and predictor variables, respectively. In order to determine the effect of the added nutrients on soil GHG fluxes (CO_2, CH_4, and N_2O), soil CO_2 sources (heterotrophic and autotrophic), and soil environmental controls (water filled pore space, soil temperature, and nitrates), LMEMs were employed. LMEMs effectively deal with temporal pseudo-replication (coming from repeated measurements) hence safeguard against inflation of the degrees of freedom, which would significantly compromise the power of the statistical

280 test. Added nutrients (treatments), seasons (wet and dry), CO_2 sources (autotrophic and heterotrophic) and phases (transitory and background) were included in the LMEMs as fixed effects while sampling days and replicate plots were included as random effects. Some of the LMEMs were extended to either include a variance function (to account for variation in the response variable per level of the fixed effect), or a first order temporal auto regressive process (to control for correlation between closely spaced measurements in time) or both. The extensions were included in the

285 LMEMs on the premise that they improved the relative goodness of model fit based on Akaike Information Criteria (AIC).

All the statistical data analyses were performed using R 3.6.3 (R Development Core Team, 2019) using *nlme' and 'car'* packages for LMEMs and one-way ANOVA tests, respectively. Throughout the paper, statistical significance in all the tests was inferred if *p ≤ 0.05*. Annual soil GHG fluxes were estimated through a trapezoidal interpolation on the

290 measured monthly soil GHG fluxes.

3 Results

3.1 Soil physico-chemical characteristics, water filled pore space, soil temperature and nitrates

Soil characteristics did not significantly differ across plots; hence, the parameters presented in Table 1 represent the soil physico-chemical characteristic for the NME site.

Table 1. Soil physico-chemical properties in three depths and vegetation characteristics of the study site located in Budongo forest, northwestern Uganda.

Soil physico-chemical properties	Soil depth (m)		
	0 - 0.10	0.10 - 0.30	0.30 - 0.50
Soil bulk density (g cm^{-3})	1.2 ± 0.2	1.5 ± 0.2	1.3 ± 0.2
Soil pH (1:2.5)	6.4 ± 0.2	6.2 ± 0.2	6.0 ± 0.2
Soil total carbon (C) (kg C m^{-2})	4.1 ± 0.0	3.1 ± 0.0	1.8 ± 0.0
Soil total nitrogen (N) (g N m^{-2})	423 ± 1.0	387 ± 0.2	249 ± 0.6
Soil C/N ratio	9.5 ± 0.3	8.0 ± 0.3	7.2 ± 0.3
Sand (%)	55 ± 2	55 ± 2	49 ± 1
Silt (%)	27 ± 2	21 ± 1	14 ± 1
Clay (%)	18 ± 1	23 ± 1	38 ± 1
ECEC (mmol$_c$ kg^{-1})	149 ± 8	76 ± 4	62 ± 4
Exchangeable aluminum (g Al m^{-2})	0.10 ± 0.06	0.11 ± 0.15	0.14 ± 0.20
Exchangeable calcium (g Ca m^{-2})	75.6 ± 4.10	39.0 ± 8.51	34.7 ± 8.59
Exchangeable magnesium (g Mg m^{-2})	17.0 ± 0.90	12.3 ± 2.7	11.7 ± 1.0
Bray II extractable phosphorus (g P m^{-2})	1.80 ± 0.20	1.01 ± 0.14	0.838 ± 0.159
Base saturation (%)	99 ± 1	97 ± 1	98 ± 1
Plant-available phosphorus (g P m^{-2})	1.7 ± 0.0	-	-
Plant-available molybdenum (mg Mo m^{-2})	14 ± 5.0	-	-
Vegetation characteristics (≥ 10 cm DBH)			
Forest type	Moist semi-deciduous tropical forest		
Most abundant tree species	Funtumia elastica, Celtis mildbraedii, Cynometra alexandri, Celtis zenkeri		
Stand height (m)	18.7 ± 0.1		
Mean basal area (m^2 ha^{-1})	34.0 ± 1.0		
Tree density (trees ha^{-1})	621 ± 13		
N fixing trees at the site (trees ha^{-1})	~ 42		

Notes: DBH is diameter at breast height. ECEC is effective cation exchange capacity.

The soils have a high bulk density (specifically 10 - 30 cm), slightly acidic pH, sandy texture, relatively high effective cation exchange capacity (ECEC), high base saturation (dominated by Ca and Mg), low in plant available phosphorus, and a low C/N (Table 1). Water filled pore space (WFPS) was significantly higher in the wet season (March to December; 55 ± 1.0 %) compared to the dry season (January to February; 43 ± 1.7 %) (Fig. 1a, Fig. 2a, $p < 0.01$). WFPS was higher in N and N + P addition plots compared the control plots both in the dry (N; $p = 0.02$, N + P; $p = 0.04$) and wet (N; $p = 0.02$, N + P; $p = 0.05$) seasons (Fig. 1a). Soil temperature varied minimally (0.6 °C) across treatments and seasons ranging between 20.1 and 21.4 °C in the dry season, and between 19.7 and 22.9 °C in the wet season. Soil nitrate contents measured across all treatment plots were significantly larger in the dry season compared to the wet season (Fig. 1c, $p < 0.01$). Soil nitrate content from the N ($p = 0.01$) and N + P ($p = 0.02$) addition plots was significantly higher than the control plots in the wet season (Fig.1c), but no significant difference was detected between the nutrient addition treatments and the control in the dry season (Fig. 1c). Strong nitrate peaks were observed in N and N + P addition plots in September 2019 and June 2020 shortly after fertilization (Fig. 2c).

Table 2. Mean (± SE, n = 4) soil GHG fluxes (CO₂, CH₄, N₂O) as well as annual soil GHG fluxes measured between May 2019 and June 2020 from control (Ctrl), nitrogen (N), phosphorus (P), and N + P plots of the nutrient manipulation experiment.

Treatment [a]	CO_2 fluxes (mg C m^{-2} h^{-1})	Annual CO_2 fluxes† (Mg C ha^{-1} yr^{-1})	CH_4 fluxes (µg C m^{-2} h^{-1})	Annual CH_4 fluxes† (kg C ha^{-1} yr^{-1})	N_2O fluxes (µg N m^{-2} h^{-1})	Annual N_2O fluxes† (kg N ha^{-1} yr^{-1})
Ctrl	164 ± 5.3[a]	14.5 ± 0.6[a]	-30.5 ± 4.9[a]	-2.7 ± 0.4[a]	20.5 ± 3.2[a]	1.8 ± 0.3[a]
N	186 ± 6.5[a]	16.4 ± 0.9[a]	-39.7 ± 4.4[a]	-3.4 ± 0.4[a]	50.2 ± 11[b]	4.8 ± 1.5[b]
P	186 ± 5.3[a]	16.4 ± 1.0[a]	-56.2 ± 3.8[b]	-4.7 ± 0.7[b]	21.8 ± 2.4[a]	1.9 ± 0.3[a]
N + P	197 ± 5.4[b]	17.3 ± 0.8[b]	-39.3 ± 6.3[a]	-3.3 ± 0.7[a]	53.8 ± 10[b]	4.6 ± 0.4[b]

Notes: [a]Means followed by different lower-case letters indicate significant differences among treatments (One way analysis of variance, $p \leq 0.05$); †Annual soil CO_2 fluxes, CH_4 fluxes, and N_2O fluxes were approximated by applying the trapezoid rule on time intervals between measured flux rates. The mean and annual soil GHG fluxes included both transitory and background flux measurements. Note: Transitory N_2O fluxes (measured within 28 days from fertilization) from N addition plots (N, N + P) were detrended to compensate for absence of frequent measurements immediately after fertilization coming from sampling GHGs monthly.

3.2 Soil CO₂ fluxes

Soil CO_2 fluxes varied between 60 and 330 mg C m^{-2} h^{-1} during the measurement period across all treatments. However, the highest CO_2 fluxes were measured in December at the interface between wet and dry season (Fig. 3a). Fertilization resulted in an immediate increase in CO_2 fluxes across all nutrient addition plots (N; 15 %, P; 14 %, N + P; 24 %) in the transitory phase. However, this increase was only significant in the N + P plots (Fig. 4a, $p = 0.01$). There was no significant effect of fertilization on background CO_2 fluxes between nutrient addition treatments and the control plots (Fig. 4d).
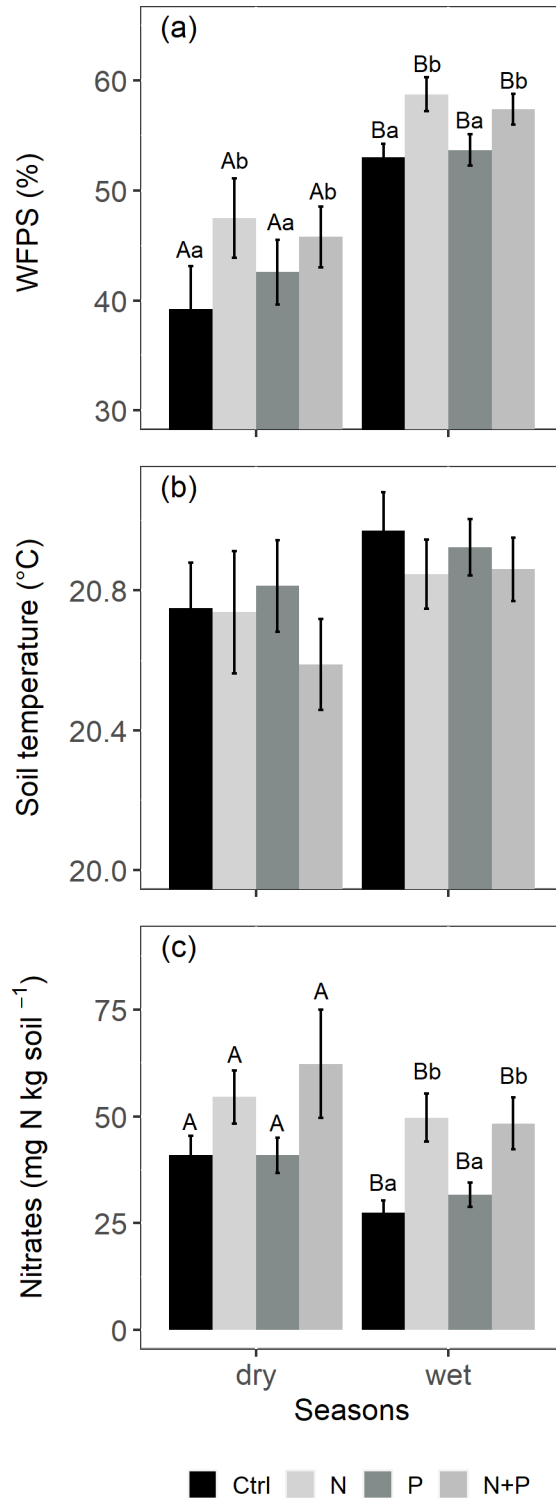
Figure 1. Mean (± SE, n = 4) water filled pore space (WFPS) (a), soil temperature (b), and nitrates (c) in the top 0.05 m of the control (Ctrl), nitrogen (N), phosphorus (P), and N + P plots of the nutrient manipulation experiment measured during the dry (January and February; monthly precipitation < 100 mm) and wet (March to December; monthly precipitation >

335   Similarly, no significant differences in the background CO_2 fluxes were detected between seasons despite measuring marginally lower background CO_2 fluxes in the wet season compared to the dry season (Fig. 4d). Additionally, no significant differences were detected between transitory and background CO_2 fluxes (Fig. 4a, d). Heterotrophic (microbial) CO_2 effluxes were significantly higher than the autotrophic (root) CO_2 effluxes (Fig. 5, $p < 0.01$) across all treatment plots with microbes contributing about three times more to the total soil CO_2 effluxes compared to roots

340   (Fig. 5, $p < 0.01$). Neither heterotrophic nor autotrophic respiration significantly differed between treatments (Fig. 5). Overall, there was relatively low variability in annual CO_2 fluxes across treatments (CV = 14.8 ± 2.2 %). The Spearman's correlation coefficient indicated that background soil CO_2 fluxes did not correlate to any of the measured soil environmental controls (WFPS, soil temperature, and nitrates) across all treatment plots (Fig. 6a, b, c).

345   **3.3   Soil CH_4 fluxes**

        Across all treatments, phases (transitory and background) and seasons, soil CH_4 fluxes varied between an uptake of -278 mg C m^{-2} h^{-1} and a release of 77 mg C m^{-2} h^{-1}. In the transitory phase, CH_4 consumption increased slightly but not significantly in the N (2 %) and N + P (6 %) plots. A larger but still not significant increase was found in the case of P plots (54 %; $p = 0.05$) (Fig. 4b). Beyond 28 days from fertilization, no significant difference in background soil CH_4

350   fluxes between treatments was detected in the dry season (Fig. 4e). However, a significantly higher background soil CH_4 consumption was measured in P plots in the wet season (Fig. 4e, $p = 0.01$). Soil CH_4 consumption in the dry season was on average 1.5 times larger than the wet season across all treatments (Fig. 4e, $p = 0.01$). Soil CH_4 uptake across all treatment plots measured during the transitory phase (-39.0 ± 3.7 mg C m^{-2} h^{-1}) did not significantly differ from the CH_4 uptake in the background phase (-42.8 ± 3.4 mg C m^{-2} h^{-1}) (Fig. 4b, e). Annual CH_4 uptake ranged

355   between -2.7 and -4.7 kg C ha^{-1} yr^{-1}, with soils in all the treatment plots acting as net sinks for CH_4 (Table 2). The Spearman's correlation coefficient test indicated that background CH_4 fluxes were strongly and positively correlated to WFPS (Fig. 6d) while soil temperature (Fig. 6e) and nitrates (Fig. 6f) were also significant but negatively correlated.

        3.4   Soil N_2O fluxes

360   Soil N_2O fluxes across treatments, phases (transitory and background), and seasons varied between an uptake of -18 and a release of 499 µg N m^{-2} h^{-1}. A strong increase of N_2O was measured immediately after fertilization (September and December 2019, April and June 2020) in all N addition plots with increases of 445 % in N plots ($p < 0.01$) and 455 % in the N + P plots ($p < 0.01$) compared to the control plots in the transitory phase (Fig. 4c). The soil N_2O peaks in September 2019 and June 2020 (Fig. 3c) coincided with the peaking in soil nitrate concentrations (Fig. 2c).

365   Background soil N_2O fluxes did not differ significantly between nutrient addition plots and the control plots both in the dry and wet seasons (Fig. 4f). Annual N_2O fluxes ranged between 1.8 and 4.8 kg N ha^{-1} yr^{-1}, with soils in all the treatment plots acting as net sources for N_2O (Table 2). The Spearman's correlation coefficient indicated that background soil N_2O fluxes were strongly and positively correlated to WFPS (Fig. 6g) in all treatment plots. Majority

of the background soil N₂O fluxes higher than 15 µg N m⁻² h⁻¹ (constituting 74 % of the averages background soil N₂O

370   fluxes) corresponded to WFPS greater than 49 % (wetter conditions) (Fig. 6g). Background soil N₂O fluxes negatively

correlated to soil temperature (Fig. 6h) and nitrates (Fig. 6i) in all treatment plots.
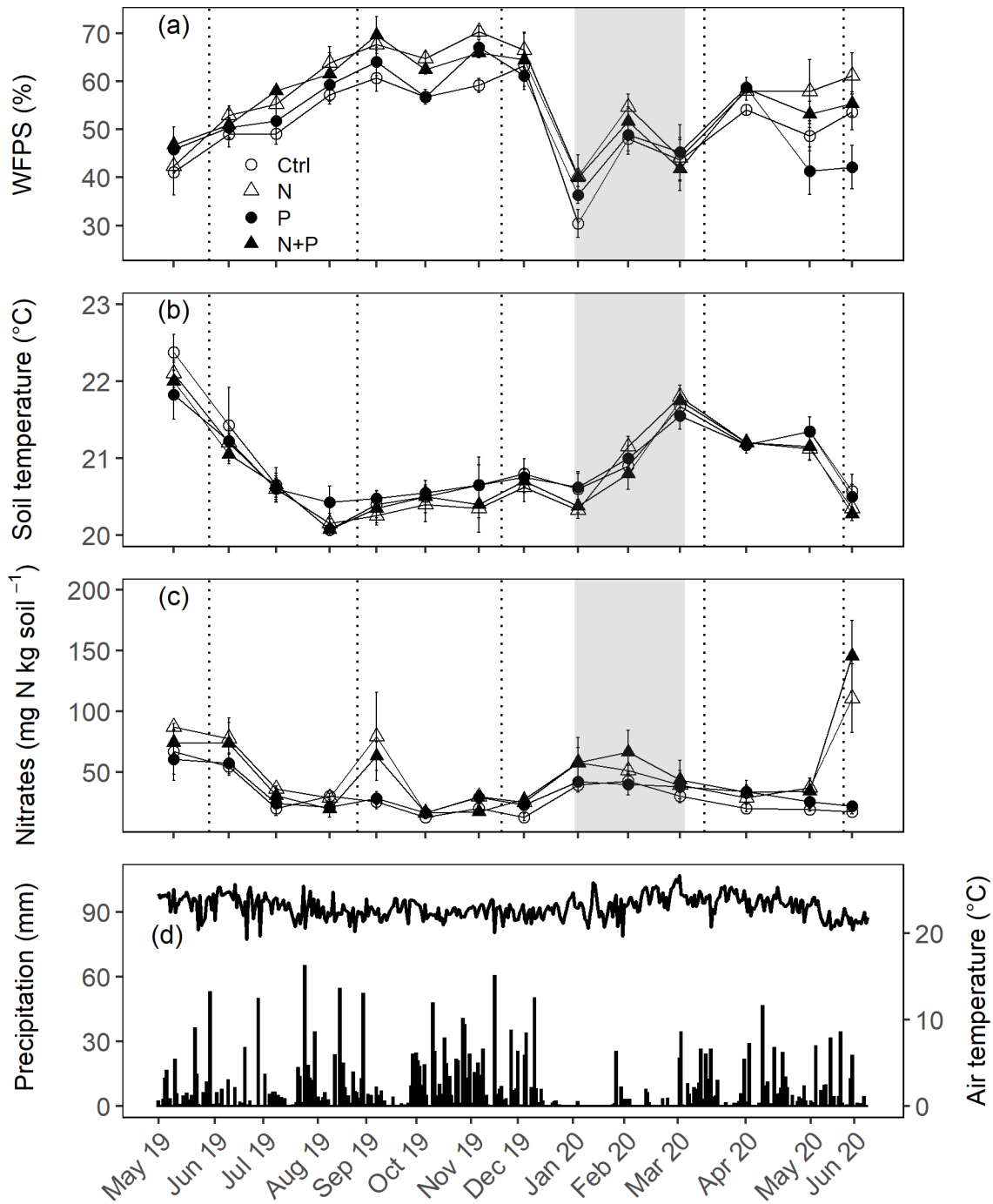
Figure 2. Mean (± SE, n = 4) water filled pore space (a), soil temperature (b), and nitrates (c) in the top 0.05 m measured monthly (May 2019 to June 2020) from control (Ctrl), nitrogen (N), phosphorus (P), and N + P plots of the nutrient

375   **manipulation experiment. Vertical lines indicate the timing of each split dose of N (31.3 kg N ha⁻¹), P (12.5 kg P ha⁻¹) and N**

(31.3 kg N ha⁻¹) + P (12.5 kg P ha⁻¹) fertilization every three months. The gray shaded rectangle (in a, b, and c) marks the beginning and end of the dry season (January and February; monthly precipitation < 100 mm), while (d) gives the daily precipitation (bars) and air temperature (line) between May 2019 and June 2020. Climatic data was obtained from a weather station installed at Budongo Conservation Field Station, 2 km from the location of the nutrient manipulation experiment in Budongo forest, northwestern Uganda.
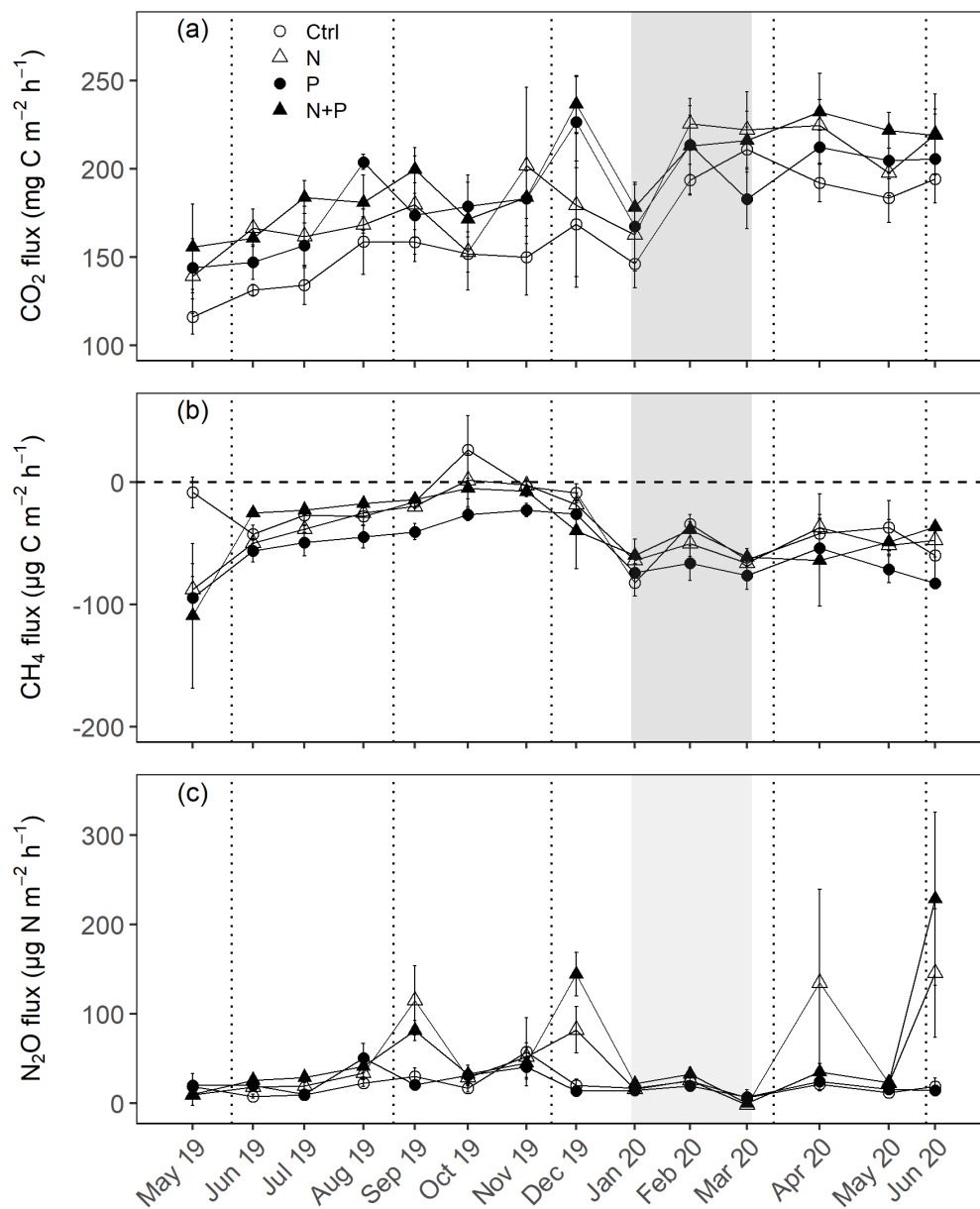
Figure 3. Mean (± SE, n = 4) soil CO₂ fluxes (a), CH₄ fluxes (b), and N₂O fluxes (c) measured monthly (between May 2019 and June 2020) from control (Ctrl), nitrogen (N), phosphorus (P), and N + P plots of the nutrient manipulation experiment. Vertical lines indicate the timing of each split dose of N (31.3 kg N ha⁻¹), P (12.5 kg P ha⁻¹) and N (31.3 kg N ha⁻¹) + P (12.5 kg P ha⁻¹) fertilization every three months. The gray shaded rectangle marks the beginning and end of the dry season (January and February; monthly precipitation < 100 mm). Note: Transitory N₂O fluxes (measured within 28 days from

fertilization) from N addition plots (N, N + P) were detrended to compensate for absence of frequent measurements immediately after fertilization coming from sampling GHGs monthly.

390 **4   Discussion**

4.1   Effect of N and P addition and soil environmental controls on soil CO_2 fluxes

The annual soil CO_2 effluxes from control plots (Table 2) were lower than those measured from tropical forests in Thailand (Hashimoto et al., 2004) and Hawaii (Townsend et al., 1995); within range to those from the Democratic Republic of Congo (Baumgartner et al., 2020), Panama (Koehler et al., 2009a; Pendall et al., 2010), Brazil (Sousa Neto

395 et al., 2011), and Cameroon (Verchot et al., 2020); and higher than those reported from Kenya (Wanyama et al., 2019), and Indonesia (van Straaten et al., 2011). The differences in soil CO_2 fluxes between the control plots in this study and studies done in other tropical forest sites may be due to differences in soil environmental characteristics e.g. soil C quality and quantity, soil temperature, and moisture availability at the respective sites (Nottingham et al., 2015).

The alleviation of nutrient limitations on soil biological activity (in microbial communities and in root respiration)

400 through fertilizer addition was particularly reflected by the significant increase in transitory CO_2 effluxes following addition of both N and P together (Fig. 4a). The transitory phase (< 28 days from fertilization) is the period where addition of nutrients (N, P, N + P) is expected to result in a large pulse of microbial activities. However, the fact that the increase in soil CO_2 effluxes was significant only in plots where N and P were added simultaneously (N + P), suggests a possible co-limitation between N and P on soil biological activity (Bréchet et al., 2019). These results

405 seemingly align with the proposed multiple element limitation concept, which suggests a strong response in microbial mediated processes upon supply of limiting nutrients (Fanin et al., 2015). Furthermore, the results likely indicate that some soil respiration sources may respond positively to N addition (Yan et al., 2017), while others may respond positively to P addition (Ma et al., 2020), yielding an overall additive response when added together. An increase in soil CO_2 effluxes following addition of N and P simultaneously together has also been reported in studies like Bréchet

410 et al. (2019), and Soong et al. (2018) from Panamanian tropical forests.

In contrast, the lack of significant treatment effects on background soil CO_2 efflux (Fig. 4a, d) and its different components (heterotrophic and autotrophic; Fig. 5) may suggest that numerous counteracting processes could be happening at the same time, hence masking treatment effects. Some studies have for instance demonstrated that addition of N subdues exoenzymes (Li et al., 2018), decreases microbial biomass (Burton et al., 2004; Hicks et al.,

415 2019), increases net primary productivity (Adamek et al., 2009), reduces fine root biomass (Cusack et al., 2011), while other studies have reported that P addition increases soil organic matter decompsition in tropical forest ecosytems (Cleveland and Townsend, 2006). The possibility of counteracting processes at the experimental site is further exemplified by the lack of a relationship between all the measured soil environmental controls (soil temperature, nitrates and soil moisture) and background CO_2 effluxes (Fig 6a, b, c). Although these results are consistent with the

420 findings by Baumgartner et al. (2020) in the Congo basin, they contrast several GHG studies located in tropical forests that have reported a strong correlation between CO_2 effluxes and soil moisture (Matson et al., 2017; van Straaten et al., 2011). For this experiment site, it could be that the minimal temporal fluctuation in soil temperature (Fig. 1b),

together with the fact that water filled pore space was mostly > 40 % (Fig. 1a) during the sampling campaign dampened the effect of soil temperature and moisture on soil CO_2 fluxes.

425
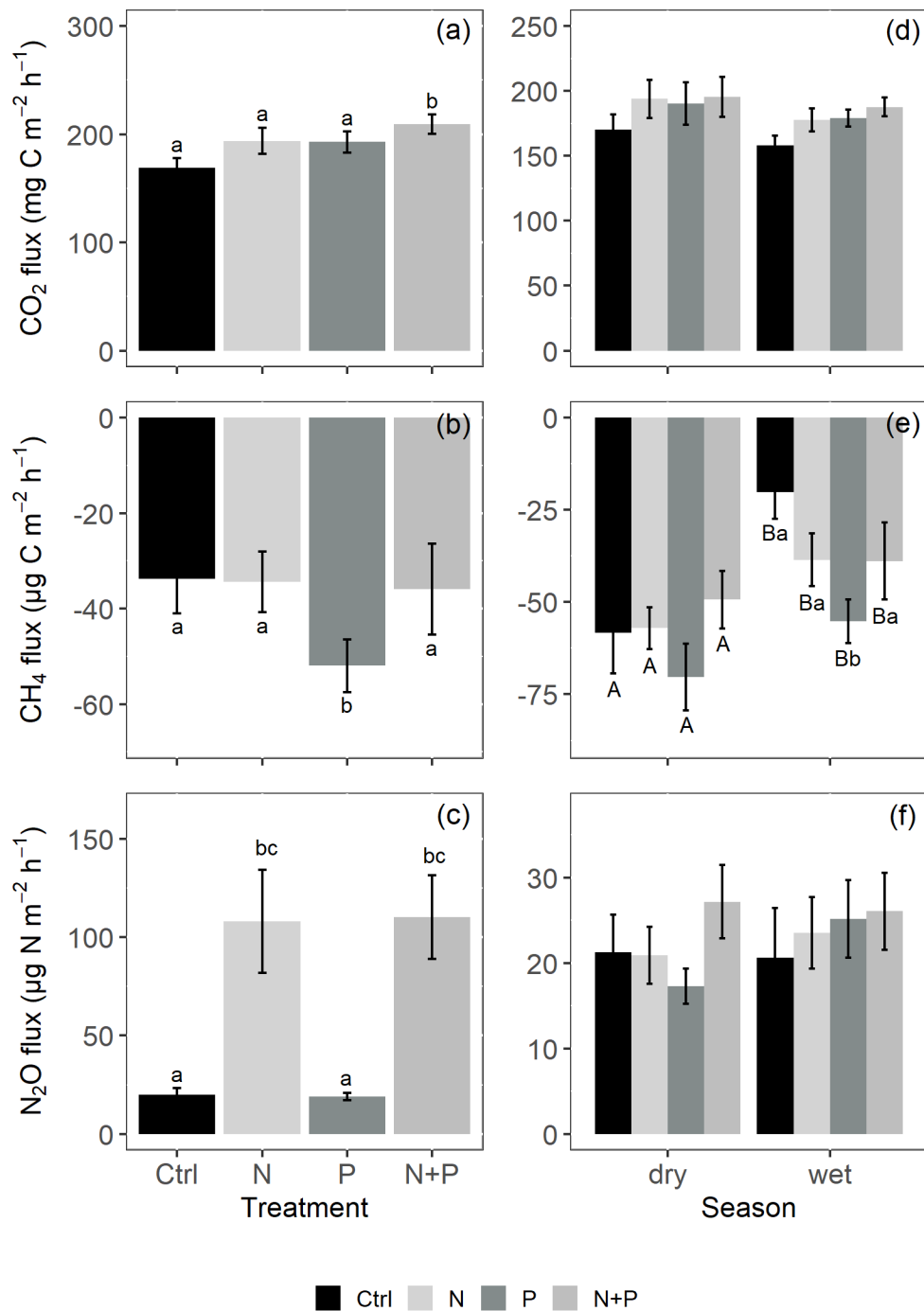
Figure 4. Mean (± SE, n = 4) soil CO_2 fluxes (a, d), CH_4 fluxes (b, e), and N_2O fluxes (c, f) from the control (Ctrl), nitrogen (N), phosphorus (P), and N + P plots of the nutrient manipulation experiment. Column 1 (a, b, and c) includes only fluxes measured during the transitory phase (0 to 28 days after fertilization; and all the transitory fluxes were in the wet season

430 (monthly precipitation >100 mm)). Column 2 (d, e, and f) includes only background level fluxes (fluxes measured more than 28 days after fertilization). Different lower-case letters indicate significant differences between nutrient addition treatments and the control while different upper-case letters indicate significant differences between seasons (linear mixed effects models; $p \leq 0.05$). Note: Transitory N_2O fluxes (measured within 28 days from fertilization) from N addition plots (N, N + P) were detrended to compensate for absence of frequent measurements immediately after fertilization coming from 435 sampling GHGs monthly.
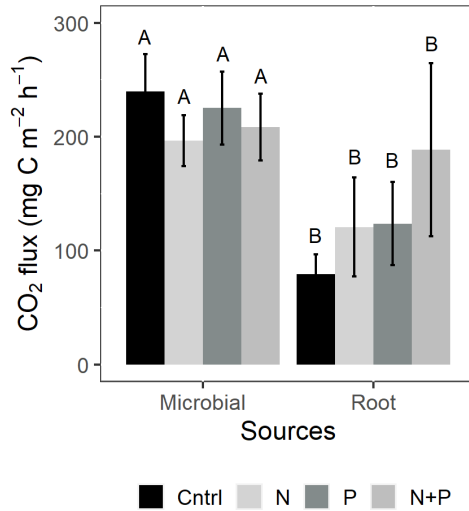
Figure 5. Mean ($\pm$ SE, n = 4) soil CO_2 flux from the control (Ctrl), nitrogen (N), phosphorus (P), and N + P plots of a trenching
440 **treatment separated into microbial and root sources. Different upper-case letters indicate significant differences between microbial and root contribution to total CO_2 flux (linear mixed effects models; $p \leq 0.05$).**

4.2 Effect of N and P addition and soil environmental controls on soil CH_4 fluxes

The annual soil CH_4 fluxes from the control plots (Table 2) were at the upper end of CH_4 fluxes measured in lowland
445 tropical forests (Aronson et al., 2019; Veldkamp et al., 2013; Zheng et al., 2016), and at the lower end of those measured in (sub-) montane tropical forest ecosystems (Sousa Neto et al., 2011; Yan et al., 2008). The difference in soil texture and soil moisture regimes between this experimental site and the other study sites might explain why CH_4 uptake at the respective sites was different. It is recognized that soil physical properties, particularly texture (Sousa Neto et al., 2011), along with soil moisture content directly control the entry and diffusivity of CH_4 from the atmosphere to the
450 oxidative sites in the soil (Veldkamp et al., 2013).

In this experiment, the significantly higher CH_4 consumption from the P addition plots compared to the control during both the transitory and background periods (Fig. 4b, e) is attributed to the alleviation of P limitations affecting methanotrophic activity. Similar findings were reported by Zhang et al. (2011), and Yu et al. (2017), but contrasted those of Bréchet et al. (2019) and Zheng et al. (2016). It is worth noting that although all these studies were located in
455 tropical forests, they differed fundamentally in their experimental designs, type and amount of fertilizers applied, and

the frequency of fertilizer application, which could have influenced the reported CH_4 uptake rates at the respective sites.

The lack of a response in background CH_4 consumption following N fertilization (Fig. 4e) is likely because there were contrasting ecosystem responses to N addition. On the one hand, the addition of nitrogen significantly increased soil

460   water filled pore space in comparison to the control (Fig. 1a; possibly as a result of reduced fine root biomass (Cusack et al., 2011)), which could have resulted in a decrease in methane uptake. On the other hand, the negative correlation between nitrates and background CH_4 fluxes (Fig. 6f) indicates that increases in soil nitrate content should increase CH_4 uptake. Additionally, the lack of a clearer signal in background CH_4 uptake may have to do with the high variability in the measured CH_4 fluxes (CV = 97 ± 58 %) potentially caused by localized termite activity (Brune, 2014;

465   Nauer et al., 2018).
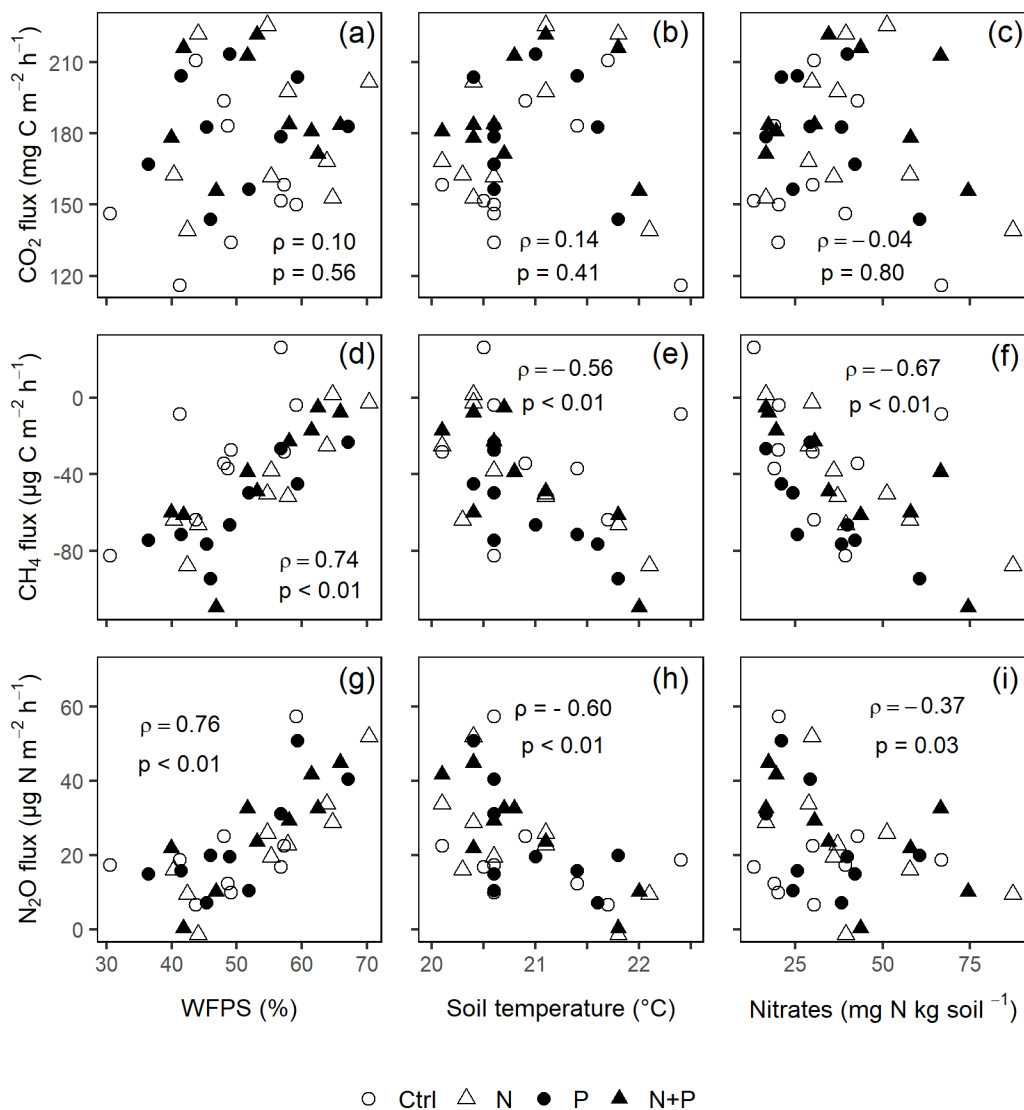
Figure 6. Spearman's correlation coefficient between mean background CO_2 (a-c), CH_4 (d-f), and N_2O (g-i) fluxes and WFPS (column 1), soil temperature (column 2) and nitrates (column 3) using monthly measurement means of four replicate

 treatment plots taken between May 2019 and June 2020 ($p \leq 0.05$, n = 16 (four replicate plots in each of the four treatments)) . ρ is the spearman's correlation coefficient.

4.3 Effect of N and P addition and soil environmental controls on soil N$_2$O fluxes

The annual soil N$_2$O fluxes from the control plots (Table 2) were at the higher end of those measured in (sub-) montane tropical forests (Iddris et al., 2020, Arias-Navarro et al., 2017, Gütlein et al., 2018), and at the lower end of those measured in lowland tropical forest sites (e.g. Koehler et al., 2009b). This may either be due to the differences in soil N cycling rates (Koehler et al., 2009b) or the differences in spatial abundance of leguminous trees (Xu et al., 2020) at the respective sites.

The immediate flush of N$_2$O following fertilization (in the transitory phase) both in the N and N + P addition plots (Fig. 3c, Fig. 4c), is due to the increase in soil N concentrations beyond microbial immobilization and plant N needs (Davidson et al., 2000), which is typical of an open or leaky N cycle (Koehler et al., 2009b). Contrary to Kaspari et al. (2008) and Koehler et al. (2009b), sustained N fertilization did not trigger a significant response in background soil N$_2$O fluxes from N addition plots (Fig. 4f). This was unexpected, but given the rapid drainage at the site (sandy texture, Table 1), there could have been substantial loss of added N via leaching, which possibly rid the ecosystem of excess nitrates (Lohse and Matson, 2005; Martinson et al., 2013). Notably, sustained P addition did not result in increased background N$_2$O fluxes (Fig. 4f), which contrasts the findings by Mori et al. (2017) who reported that P availability opens up the N cycle by stimulating mineralization of soil organic matter releasing excess N that is lost as N$_2$O emissions. At this study site, it could be that either the amount of P added in the experiment was not sufficient to trigger a response in background soil N$_2$O fluxes or P is not a limiting nutrient for N$_2$O fluxes given the relatively high pH of the site (Table 1).

Unexpectedly, nitrates correlated negatively to background N$_2$O fluxes (Fig. 6i), yet many studies (e.g. Corre et al., 2014; Zhang et al., 2020) have found that nitrates and N$_2$O fluxes were positively correlated. The likely explanation for such a relationship is the transformation of N$_2$O to N$_2$ under wet conditions, which further reduced the amount of nitrates in soil (Matson et al., 2017). Despite the minimal influence of seasonality on background N$_2$O fluxes (Fig. 4f), a strong positive correlation between background N$_2$O fluxes and WFPS was observed (Fig 6g), which conforms to the explanation given by the conceptual hole in the pipe (HIP) model. The HIP model places soil aeration status (approximated by WFPS) second to N availability in controlling soil N$_2$O fluxes. Soil aeration not only directly controls oxygen entry into the soil but also determines how N$_2$O is produced (denitrification or nitrification), and transported out of the soil (Davidson et al., 2000). Whereas there seems to be a balance between denitrification and nitrification process at this forest site (given that majority of the measurements corresponded to WFPS of ≤ 60 %, Fig. 6g), the considerable N$_2$O fluxes at higher WFPS values (≥ 60 %, Fig. 6g) seem to suggest that denitrification is more dominant than nitrification in producing N$_2$O in these biomes.

4.4 Implications of increasing N and P deposition rates on soil greenhouse gases from tropical forests

While this experiment was established to investigate how nutrient limitations constrain soil GHG fluxes, it also sheds valuable insights on how anthropogenic nutrient inputs (through deposition) may affect future soil GHG fluxes from

African tropical forests and other tropical sites with a similarly strong seasonality, soil, and vegetation characteristics (Table 1). Nutrient depositions are often highest immediately after the onset of the rainy season (Wang et al., 2020), especially due to aerosol deposition following burning activities associated with deforestation during the dry season (Giglio et al., 2006; Roberts et al., 2009). Accordingly, we suspect that the increased N inputs during this short time may yield similar responses to those observed in the transitory period measured at this study site; namely—N_2O flushes when reactive nitrogen enters the soil. Although N additions did not elicit a positive N_2O response during the background period, it is quite likely that our fertilization activities (from year 1 to year 2 of the study) had not gone on for long enough to simulate chronic long-term N additions. A study conducted by Koehler et al. (2009b) in Panama showed that 11 years of chronic N addition significantly increased both transitory and background soil N_2O emissions. In addition, this study shows that future increases in P deposition over tropical forests may significantly increase the CH_4 sink capacity of tropical forest soils. Also, it was interesting to observe that the addition of N and P simultaneously resulted in increased CO_2 effluxes immediately after fertilization likely suggesting a co-limitation of N and P on soil respiration. This means that future increases in deposition of N and P rich ashes (from biomass burning), might result in significant soil CO_2 emissions from these biomes, while it is unclear if this is compensated via an increase in photosynthetic CO_2 uptake as indicated by Cernusak et al. (2013). In this context, it is important to note that it has been demonstrated by Barkley et al. (2019) that P derived from biomass burning aerosols is more soluble than the P from dust aerosols, hence, the former would have an immediate impact on ecosystem processes.

5. Conclusion

Nutrient manipulation studies premised in tropical forests are crucial to understand how these under-studied yet very important sinks and sources of soil GHGs subtly respond to changes in soil macro nutrient availability. N fertilization (N and N + P) significantly increased N_2O fluxes immediately after fertilization (transitory phase), but had no significant effect on background N_2O fluxes, which might occur if the system would gain N over longer time spans. Against our expectations, neither background CO_2 effluxes nor CH_4 uptake decreased following addition of N, indicating neither a negative effect of a potential surplus of soil N on root and microbial respiration nor a negative effect on methanotrophs. CO_2 effluxes even showed a significant increase during the transitory phase following N and N + P fertilization. However, this effect was only significant for N + P addition, indicating some N and P co-limitation. An increase in CH_4 uptake was found both shortly and after sustained P fertilization; supporting our second hypothesis, which suggested that lifting the P limitation on soil methanotrophs, would significantly increase CH_4 consumption. Surprisingly, both transitory and background N_2O and CO_2 fluxes (including its different components) were not significantly affected by P fertilization. Overall, the results from this first nutrient manipulation GHG study from a wet African tropical forest site, in general, indicate our limited knowledge about the counteracting interactions between N and P inputs and GHG fluxes from different tropical forest ecosystems. This confines any general conclusions and equally limits our ability to parametrize tropical forest ecosystems in Earth System Models. Nevertheless, the contribution of tropical forest biomes to the global soil GHG budgets maybe disproportionately altered via potential future increases in N and P availability.

Declaration on Conflict of Interest. We declare that there is no conflict of interest.

545

Author contribution. JT and OvS conceptualized the study. OvS established the nutrient manipulation experiment. JT conducted the fieldwork, did data analysis and prepared the manuscript. OvS, PF, and SD provided significant input on the experimental set-up and data analysis. RH and BM did laboratory measurements and gave critical feedback on the manuscript. OvS, PF, SD, MG, and LFT critically reviewed and gave feedback on the manuscript.

550

Data availability. Data is available on request.

Acknowledgement. We thank F. Babweteera and Budongo Conservation Field Station management for hosting the nutrient manipulation experiment, providing us with working space and the climatic data. Special thanks goes to Johan
555 Six's laboratory ETH-Zürich for analyzing the gas samples. We are grateful to the German Academic Exchange (DAAD) (grant number: 57381412) for JT's stipendium and meeting his travel costs between Uganda and Germany. We also thank the International Foundation of Science (IFS), Stockholm, Sweden, for the financial support (grant number: D/6293-1) towards JT's fieldwork in Uganda, and the National Agricultural Research Organization (NARO) for the institutional support and administration of the IFS grant. We thank the DFG funded Emmy Noether Junior
560 Research Group "TropSOC" (Gepris - project number 387472333) for the additional support towards this study and the DFG funded Individual Research project (RELIANCE; grant number STR 1375/1-1) for setting up the nutrient manipulation experiment. Lastly, we thank G. B. Ayo and M. Adriko for supporting our field measurements.

References

565 Adamek, M., Corre, M. D. and Hölscher, D.: Early effect of elevated nitrogen input on above-ground net primary production of a lower montane rain forest, Panama, J. Trop. Ecol., 256, 637–647, doi:10.1017/S0266467409990253, 2009.

Arias-Navarro, C., Díaz-Pinés, E., Kiese, R., Rosenstock, T. S., Rufino, M. C., Stern, D., Neufeldt, H., Verchot, L. V. and Butterbach-Bahl, K.: Gas pooling: A sampling technique to overcome spatial heterogeneity of soil carbon dioxide
570 and nitrous oxide fluxes, Soil Biol. Biochem., 67, 20-23, doi:10.1016/j.soilbio.2013.08.011, 2013.

Arias-Navarro, C., Díaz-Pinés, E., Zuazo, P., Rufino, M. C., Verchot, L. V. and Butterbach-Bahl, K.: Quantifying the contribution of land use to N_2O, NO and CO_2 fluxes in a montane forest ecosystem of Kenya, Biogeochemistry., 134, 95–114, doi:10.1007/s10533-017-0348-3, 2017.

Aronson, E. L. and Helliker, B. R.: Methane flux in non-wetland soils in response to nitrogen addition: A meta-analysis,
575 Ecology., 91, 3242–3251, doi:10.1890/09-2185.1, 2010.

Aronson, E. L., Dierick, D., Botthoff, J. K., Oberbauer, S., Zelikova, T. J., Harmon, T. C., Rundel, P., Johnson, R. F., Swanson, A. C., Pinto-Tomás, A. A., Artavia-León, A., Matarrita-Carranza, B. and Allen, M. F.: ENSO-influenced drought drives methane flux dynamics in a tropical wet forest soil, J. Geophys. Res., 124, 2267–2276, doi:10.1029/2018JG004832, 2019.

580 Barkley, A. E., Prospero, J. M., Mahowald, N., Hamilton, D. S., Popendorf, K. J., Oehlert, A. M., Pourmand, A., Gatineau, A., Panechou-Pulcherie, K., Blackwelder, P. and Gaston, C. J.: African biomass burning is a substantial source of phosphorus deposition to the Amazon, Tropical Atlantic Ocean, and Southern Ocean, Proc. Natl. Acad. Sci. U. S. A., 116(33), 16216–16221, doi:10.1073/pnas.1906091116, 2019.

Baumgartner, S., Barthel, M., Drake, T., Bauters, M., Makelele, I. A., Mugula, J. K., Summerauer, L., Gallarotti, N., 585 Ntaboba, L. C., Van Oost, K., Boeckx, P., Doetterl, S., Werner, R. and Six, J.: Seasonality, drivers, and isotopic composition of soil CO_2 fluxes from tropical forests of the Congo Basin, Biogeosciences., 17, 6207–6218, doi:10.5194/bg-17-6207-2020, 2020.

Bauters, M., Verbeeck, H., Rütting, T., Barthel, M., Bazirake Mujinya, B., Bamba, F., Bodé, S., Boyemba, F., Bulonza, E., Carlsson, E., Eriksson, L., Makelele, I., Six, J., Cizungu Ntaboba, L. and Boeckx, P.: Contrasting nitrogen fluxes 590 in African tropical forests of the Congo Basin, Ecol. Monogr., 89(1), 1–17, doi:10.1002/ecm.1342, 2019.

Bobbink, R., Hicks, K., Galloway, J., Spranger, T., Alkemade, R., Ashmore, M., Bustamante, M., Cinderby, S., Davidson, E., Dentener, F., Emmett, B., Erisman, J. W., Fenn, M., Gilliam, F., Nordin, A., Pardo, L. and De Vries, W.: Global assessment of nitrogen deposition effects on terrestrial plant diversity: A synthesis, Ecol. Appl., 20, 30-59, doi:10.1890/08-1140.1, 2010.

595 Bodelier, P. L. E. and Steenbergh, A. K.: Interactions between methane and the nitrogen cycle in light of climate change, Curr. Opin. Environ. Sustain., 9-10, 26-36, doi:10.1016/j.cosust.2014.07.004, 2014.

Bréchet, L., Courtois, E. A., Saint-Germain, T., Janssens, I. A., Asensio, D., Ramirez-Rojas, I., Soong, J. L., Van Langenhove, L., Verbruggen, E. and Stahl, C.: Disentangling drought and nutrient effects on soil carbon dioxide and methane fluxes in a tropical forest, Front. Environ. Sci., 7, 180, doi:10.3389/fenvs.2019.00180, 2019.

600 Brune, A.: Symbiotic digestion of lignocellulose in termite guts, Nat. Rev. Microbiol., 12, 168–180, doi:10.1038/nrmicro3182, 2014.

Burton, A. J., Pregitzer, K. S., Crawford, J. N., Zogg, G. P. and Zak, D. R.: Simulated chronic NO_3^- deposition reduces soil respiration in northern hardwood forests, Glob. Chang. Biol., 10, 1080–1091, doi:10.1111/j.1365-2486.2004.00737.x, 2004.

605 Butterbach-Bahl, K., Kiese, R. and Liu, C.: Measurements of biosphere atmosphere exchange of CH_4 in terrestrial ecosystems, 1st ed, Methods Enzymol, Elsevier Inc., 495:271-87, doi: 10.1016/B978-0-12-386905-0.00018-8, 2011.

Butterbach-Bahl, K., Kock, M., Willibald, G., Hewett, B., Buhagiar, S., Papen, H. and Kiese, R.: Temporal variations of fluxes of NO, NO_2, N_2O, CO_2, and CH_4 in a tropical rain forest ecosystem, Glob. Biogeochem. Cycles., 18, doi:10.1029/2004GB002243, 2004.

610 Cernusak, L.A., Winter, K., Dalling, J.W., Holtum, J.A., Jaramillo, C., Körner, C., Leakey, A.D., Norby, R.J., Poulter, B., Turner, B.L. and Wright, S.J.: Tropical forest responses to increasing atmospheric CO_2: current knowledge and opportunities for future research. Funct. Plant Biol., 40, 531-551, doi.org/10.1071/FP12309, 2013.Chen, D., Zhou, L., Rao, X., Lin, Y. and Fu, S.: Effects of root diameter and root nitrogen concentration on in situ root respiration among different seasons and tree species, Ecol. Res., 25, 983–993, doi:10.1007/s11284-010-0722-2, 2010.

615 Cleveland, C. C. and Townsend, A. R.: Nutrient additions to a tropical rain forest drive substantial soil carbon dioxide losses to the atmosphere, Proc. Natl. Acad. Sci. U.S.A., 103, 10316-10321, doi:10.1073/pnas.0600989103, 2006.

Corre, M. D., Sueta, J. P. and Veldkamp, E.: Nitrogen-oxide emissions from tropical forest soils exposed to elevated nitrogen input strongly interact with rainfall quantity and seasonality, Biogeochemistry., 118, 103-120, doi:10.1007/s10533-013-9908-3, 2014.

620 Corre, M. D., Veldkamp, E., Arnold, J., and Wright, S. J.: Impact of elevated N input on soil N cycling and losses in old-growth lowland and montane forests in Panama. Ecology., 91, 1715–1729, doi: 10.1890/09-0274.1, 2010.

Cusack, D. F., Silver, W. L., Torn, M. S., Burton, S. D. and Firestone, M. K.: Changes in microbial community characteristics and soil organic matter with nitrogen additions in two tropical forests, Ecology., 92, 621–632, doi:10.1890/10-0459.1, 2011.

625 Davidson, E. A., Keller, M., Erickson, H. E., Verchot, L. V. and Veldkamp, E.: Testing a conceptual model of soil emissions of nitrous and nitric oxides, Bioscience., 50, 667–680, doi:10.1641/0006-3568(2000)050[0667:TACMOS]2.0.CO;2, 2000.

DeForest, J. L., Noormets, A., McNulty, S. G., Sun, G., Tenney, G. and Chen, J.: Phenophases alter the soil respiration-temperature relationship in an oak-dominated forest, Int. J. Biometeorol., 51, 135-144, doi:10.1007/s00484-006-0046-630 7, 2006.

Doetterl, S., Stevens, A., Six, J., Merckx, R., Oost, K. Van, Pinto, M. C., Casanova-Katny, A., Muñoz, C., Boudin, M., Venegas, E. Z. and Boeckx, P.: Soil carbon storage controlled by interactions between geochemistry and climate, Nature Geoscience., 8, 780-783, doi:10.1038/NGEO2516, 2015.

Du, E., Xia, N. and de Vries, W.: Effects of nitrogen deposition on growing-season soil methane sink across global 635 forest biomes, Biogeosciences Discuss., 1–16, doi:10.5194/bg-2019-29, February, 2019.

Dutaur, L. and Verchot, L. V.: A global inventory of the soil CH_4 sink, Glob. Biogeochem. Cycles., 21, 1–9, doi:10.1029/2006GB002734, 2007.

Eggeling, W. J.: Observations on the ecology of the Budongo rainforest, Uganda, J. Ecol., 34, 20-87, doi:10.2307/2256760, 1947.

640 Fanin, N., Hättenschwiler, S., Schimann, H. and Fromin, N.: Interactive effects of C, N and P fertilization on soil microbial community structure and function in an Amazonian rain forest, Funct. Ecol., 29, 140–150, doi:10.1111/1365-2435.12329, 2015.

Galloway, J., Dentener, F., Capone, D., Boyer, E. and Howarth, R.: Nitrogen cycles: past, present, and future, Biogeochemistry., 70, 2004.

645 Giglio, L., Csiszar, I., and Justice, C. O.: Global distribution and seasonality of active fires as observed with Terra and Aqua Moderate Resolution Imaging Spectroradiometers (MODIS) sensors, J. Geophys. Res., 111, G02016, doi:10.1029/2005JG000142, 2006.

Gray, N. D., McCann, C. M., Christgen, B., Ahammad, S. Z., Roberts, J. A. and Graham, D. W.: Soil geochemistry confines microbial abundances across an arctic landscape; implications for net carbon exchange with the atmosphere, 650 Biogeochemistry., 120, 307–317, doi:10.1007/s10533-014-9997-7, 2014.

Gütlein, A., Gerschlauer, F., Kikoti, I. and Kiese, R.: Impacts of climate and land use on N_2O and CH_4 fluxes from tropical ecosystems in the Mt. Kilimanjaro region, Tanzania, Glob. Chang. Biol., 24, 1239–1255, doi:10.1111/gcb.13944, 2018.

Hall, S. J., and Matson P. A.: Nutrient status of tropical rain forests influences soil N dynamics after N additions. Ecological Monographs., 73, 107–129, jstor.org/stable/3100077, 2003.

Hashimoto, S., Tanaka, N., Suzuki, M., Inoue, A., Takizawa, H., Kosaka, I., Tanaka, K., Tantasirin, C. and Tangtham, N.: Soil respiration and soil CO_2 concentration in a tropical forest, Thailand, J. For. Res., 9, 75–79, doi:10.1007/s10310-003-0046-y, 2004.

Hassler, E., Corre, M. D., Tjoa, A., Damris, M., Utami, S. R., and Veldkamp, E.: Soil fertility controls soil–atmosphere carbon dioxide and methane fluxes in a tropical landscape converted from lowland forest to rubber and oil palm plantations. Biogeosciences., 12(19), 5831-5852, doi.org/10.5194/bg-12-5831, 2015.

Hedin, L.O., Vitousek, P.M. and Matson, P.A.: Nutrient losses over four million years of tropical forest development. Ecology., 84(9), 2231-2255, doi.org/10.1890/02-4066, 2003.

Hicks, L. C., Meir, P., Nottingham, A. T., Reay, D. S., Stott, A. W., Salinas, N. and Whitaker, J.: Carbon and nitrogen inputs differentially affect priming of soil organic matter in tropical lowland and montane soils, Soil Biol. Biochem., 129, 212–222, doi:10.1016/j.soilbio.2018.10.015, 2019.

Hobbie, S. E. and Vitousek, P. M.: Nutrient limitation of decomposition in Hawaiian forests, Ecology., 81, 1867-1877, doi:10.1890/0012-9658(2000)081[1867:NLODIH]2.0.CO;2, 2000.

Holland, E. A., Neff, J. C., Townsend, A. R. and McKeown, B.: Uncertainties in the temperature sensitivity of decomposition in tropical and subtropical ecosystems: Implications for models, Glob. Biogeochem. Cycles., 14, 1137-1151, doi:10.1029/2000GB001264, 2000.

Iddris, N. A.-A., Corre, M. D., Yemefack, M., van Straaten, O. and Veldkamp, E.: Stem and soil nitrous oxide fluxes from rainforest and cacao agroforest on highly weathered soils in the Congo Basin, Biogeosciences., 17, 5377–5397, doi:10.5194/bg-17-5377-2020, 2020.

IUSS Working Group WRB: World reference base for soil resources 2014. International soil classification system for naming soils and creating legends for soil maps., 106, 2014.

Jiang, X., Chen, H., Peng, C., Li, Y., He, Y., Chen, D., Lin, M., Hu, J., Ma, T., Liu, L., Liu, X., Xia, M. and Liu, Y.: Soil carbon dioxide fluxes from three forest types of the tropical montane rainforest on Hainan Island, China, Water. Air. Soil Pollut., 227, doi:10.1007/s11270-016-2904-1, 2016.

Jobbágy, E. G. and Jackson, R. B.: The vertical distribution of soil organic carbon and its relation to climate and vegetation, Ecol. Appl., 10, 423-436, doi:10.1890/1051-0761(2000)010[0423:TVDOSO]2.0.CO;2, 2000.

John, R., Dalling, J. W., Harms, K. E., Yavitt, J. B., Stallard, R. F., Mirabello, M., Hubbell, S. P., Valencia, R., Navarrete, H., Vallejo, M. and Foster, R. B.: Soil nutrients influence spatial distributions of tropical trees species, Proc. Natl. Acad. Sci. U.S.A., 104, 864-869, doi:10.1073/pnas.0604666104, 2007.

Kaspari, M., Garcia, M. N., Harms, K. E., Santana, M., Wright, S. J. and Yavitt, J. B.: Multiple nutrients limit litterfall and decomposition in a tropical forest, Ecol. Lett., 11, 35–43, doi:10.1111/j.1461-0248.2007.01124.x, 2008.

Koehler, B., Corre, M. D., Veldkamp, E. and Sueta, J. P.: Chronic nitrogen addition causes a reduction in soil carbon dioxide efflux during the high stem-growth period in a tropical montane forest but no response from a tropical lowland forest on a decadal time scale, Biogeosciences., 6, 2973–2983, doi:10.5194/bg-6-2973-2009, 2009a.

690   Koehler, B., Corre, M. D., Veldkamp, E., Wullaert, H. and Wright, S. J.: Immediate and long-term nitrogen oxide emissions from tropical forest soils exposed to elevated nitrogen input, Glob. Chang. Biol., 15, 2049–2066, doi:10.1111/j.1365-2486.2008.01826.x, 2009b.

Li, Y., Sun, J., Tian, D., Wang, J., Ha, D., Qu, Y., Jing, G. and Niu, S.: Soil acid cations induced reduction in soil respiration under nitrogen enrichment and soil acidification, Sci. Total Environ., 615, 1535–1546,
695   doi:10.1016/j.scitotenv.2017.09.131, 2018.

Li, Y., Xu, M. and Zou, X.: Effects of nutrient additions on ecosystem carbon cycle in a Puerto Rican tropical wet forest, Glob. Chang. Biol., 12, 284–293, doi:10.1111/j.1365-2486.2005.01096.x, 2006.

Lohse, K. A. and Matson, P.: Consequences of nitrogen additions for soil losses from wet tropical forests, Ecol. Appl., 15, 1629–1648, doi:10.1890/03-5421, 2005.

700   Lukwago, W., Behangana, M., Mwavu, E. N. and Hughes, D. F.: Effects of selective timber harvest on amphibian species diversity in Budongo forest Reserve, Uganda, Forest. Ecol. Manag., 458, doi:10.1016/j.foreco.2019.117809, 2020.

Ma, S., Chen, G., Tian, D., Du, E., Xiao, W., Jiang, L., Zhou, Z., Zhu, J., He, H., Zhu, B. and Fang, J.: Effects of seven-year nitrogen and phosphorus additions on soil microbial community structures and residues in a tropical forest in
705   Hainan Island, China, Geoderma., 361, 114034, doi:10.1016/j.geoderma.2019.114034, 2020.

Malhi, Y. and Phillips, O. L.: Tropical forests and global atmospheric change: A synthesis, Philos. Trans. R. Soc. B Biol. Sci., 359, 549–555, doi:10.1098/rstb.2003.1449, 2004.

Martinson, G. O., Corre, M. D. and Veldkamp, E.: Responses of nitrous oxide fluxes and soil nitrogen cycling to nutrient additions in montane forests along an elevation gradient in southern Ecuador, Biogeochemistry., 112, 625-
710   636, doi:10.1007/s10533-012-9753-9, 2013.

Matson, A. L., Corre, M. D. and Veldkamp, E.: Nitrogen cycling in canopy soils of tropical montane forests responds rapidly to indirect N and P fertilization, Glob. Chang. Biol., 20, 3802–3813, doi:10.1111/gcb.12668, 2014.

Matson, A. L., Corre, M. D., Langs, K. and Veldkamp, E.: Soil trace gas fluxes along orthogonal precipitation and soil fertility gradients in tropical lowland forests of Panama, Biogeosciences., 14, 3509–3524, doi:10.5194/bg-14-3509-
715   2017, 2017.

McGroddy, M. E., Baisden, W. T. and Hedin, L. O.: Stoichiometry of hydrological C, N, and P losses across climate and geology: An envionmental matrix approach across New Zealand primary forests, Glob. Biogeochem. Cycles., 22, doi:10.1029/2007GB003005, 2008.

Mori, T., Lu, X., Aoyagi, R. and Mo, J.: Reconsidering the phosphorus limitation of soil microbial activity in tropical
720   forests, Funct. Ecol., 32, 1145–1154, doi:10.1111/1365-2435.13043, 2018.

Mori, T., Ohta, S., Ishizuka, S., Konda, R., Wicaksono, A., Heriyanto, J. and Hardjono, A.: Effects of phosphorus application on root respiration and heterotrophic microbial respiration in Acacia mangium plantation soil, Tropics., 22, 113–118, doi:10.3759/tropics.22.113, 2013.

Mori, T., Ohta, S., Ishizuka, S., Konda, R., Wicaksono, A., Heriyanto, J. and Hardjono, A.: Effects of phosphorus
725   addition on N_2O and NO emissions from soils of an Acacia mangium plantation, Soil Sci. Plant Nutr., 56(5), 782–788, doi:10.1111/j.1747-0765.2010.00501.x, 2010.

Mosier, A., Wassmann, R., Verchot, L., King, J. and Palm, C.: Methane and nitrogen oxide fluxes in tropical agricultural soils: Sources, sinks and mechanisms, Environ. Dev. Sustain., 6, 11-49, doi:10.1023/B:ENVI.0000003627.43162.ae, 2004.

730 Müller, A. K., Matson, A. L., Corre, M. D. and Veldkamp, E.: Soil N_2O fluxes along an elevation gradient of tropical montane forests under experimental nitrogen and phosphorus addition, Front. Earth Sci., 3, 66, doi:10.3389/feart.2015.00066, 2015.

Nauer, P. A., Hutley, L. B. and Arndt, S. K.: Termite mounds mitigate half of termite methane emissions, Proc. Natl. Acad. Sci. U. S. A., 115, 13306–13311, doi:10.1073/pnas.1809790115, 2018.

735 Nottingham, A. T., Whitaker, J., Turner, B. L., Salinas, N., Zimmermann, M., Malhi, Y. and Meir, P.: Climate Warming and Soil Carbon in Tropical Forests: Insights from an Elevation Gradient in the Peruvian Andes, Bioscience., 65, 906–921, doi:10.1093/biosci/biv109, 2015.

Oertel, C., Matschullat, J., Zurba, K., Zimmermann, F. and Erasmi, S.: Greenhouse gas emissions from soils—A review, Chemie der Erde., 76, 327-352, doi:10.1016/j.chemer.2016.04.002, 2016.

740 Pavelka, M., Acosta, M., Kiese, R., Altimir, N., Brümmer, C., Crill, P., Darenova, E., Fuß, R., Gielen, B., Graf, A. and Klemedtsson, L.: Standardization of chamber technique for CO_2, N_2O and CH_4 fluxes measurements from terrestrial ecosystems, Int. Agrophys., 32, 569-587, doi: 10.1515/intag-2017-0045, 2018.

Pendall, E., Schwendenmann, L., Rahn, T., Miller, J. B., Tans, P. P. and White, J. W. C.: Land use and season affect fluxes of CO_2, CH_4, CO, N_2O and H_2 and isotopic source signatures in Panama: Evidence from nocturnal boundary

745 layer profiles, Glob. Chang. Biol., 16, 2721–2736, doi:10.1111/j.1365-2486.2010.02199.x, 2010.

R Development Core Team: a language and environment for statistical computing. R Foundation for Statistical Computing, Vienna, Austria, 2019.

Roberts, G., Wooster, M.J. and Lagoudakis, E.: Annual and diurnal African biomass burning temporal dynamics. Biogeosciences., 6(5), 849-866, doi.org/10.5194/bg-6-849-2009, 2009.

750 Saatchi, S. S., Harris, N. L., Brown, S., Lefsky, M., Mitchard, E. T. A., Salas, W., Zutta, B. R., Buermann, W., Lewis, S. L., Hagen, S., Petrova, S., White, L., Silman, M. and Morel, A.: Benchmark map of forest carbon stocks in tropical regions across three continents, Proc. Natl. Acad. Sci. U.S.A., 108, 9899-904, doi:10.1073/pnas.1019576108, 2011.

Seghers, D., Top, E. M., Reheul, D., Bulcke, R., Boeckx, P., Verstraete, W. and Siciliano, S. D.: Long-term effects of mineral versus organic fertilizers on activity and structure of the methanotrophic community in agricultural soils,

755 Environ. Microbiol., 5, 867-77, doi:10.1046/j.1462-2920.2003.00477.x, 2003.

Sjögersten, S., Aplin, P., Gauci, V., Peacock, M., Siegenthaler, A. and Turner, B. L.: Temperature response of ex-situ greenhouse gas emissions from tropical peatlands: Interactions between forest type and peat moisture conditions, Geoderma., 324, 47-55, doi:10.1016/j.geoderma.2018.02.029, 2018.

Soong, J. L., Marañon-Jimenez, S., Cotrufo, M. F., Boeckx, P., Bodé, S., Guenet, B., Peñuelas, J., Richter, A., Stahl,

760 C., Verbruggen, E. and Janssens, I. A.: Soil microbial CNP and respiration responses to organic matter and nutrient additions: Evidence from a tropical soil incubation, Soil Biol. Biochem., 122, 141–149, doi:10.1016/j.soilbio.2018.04.011, 2018.

Sousa Neto, E., Carmo, J. B., Keller, M., Martins, S. C., Alves, L. F., Vieira, S. A., Piccolo, M. C., Camargo, P., Couto, H. T. Z., Joly, C. A. and Martinelli, L. A.: Soil atmosphere exchange of nitrous oxide, methane and carbon dioxide in

765   a gradient of elevation in the coastal Brazilian Atlantic forest, Biogeosciences., 8, 733–742, doi:10.5194/bg-8-733-2011, 2011.

Tamatamah, R. A., Hecky, R. E. and Duthie, H. C.: The atmospheric deposition of phosphorus in Lake Victoria (East Africa), Biogeochemistry., 73(2), 325–344, doi:10.1007/s10533-004-0196-9, 2005.

Tanner, E. V. J., Vltousek, P. M. and Cuevas, E.: Experimental investigation of nutrient limitation of forest growth on

770   wet tropical mountains, Ecology., 79(1), 10–22, doi:10.1890/0012-9658(1998)079[0010:EIONLO]2.0.CO;2, 1998.

Townsend, A. R., Vitousek, P. M. and Trumbore, S. E.: Soil organic matter dynamics along gradients in temperature and land use on the island of Hawaii, Ecology., 76, 721–733, doi:10.2307/1939339, 1995.

van Straaten, H.P.: Präkambrium und junges Western Rift im Bunyoro Distrikt, NW- Uganda (Ostafrika), Geologishes Jahbuch. Reihe B, Heft 18. Hanover, 1976.

775   van Straaten, O., Veldkamp, E. and Corre, M. D.: Simulated drought reduces soil CO_2 efflux and production in a tropical forest in Sulawesi, Indonesia , Ecosphere., 2, 1-22, doi:10.1890/es11-00079.1, 2011.

Veber, G., Kull, A., Villa, J. A., Maddison, M., Paal, J., Oja, T., Iturraspe, R., Pärn, J., Teemusk, A. and Mander, Ü.: Greenhouse gas emissions in natural and managed peatlands of America: Case studies along a latitudinal gradient, Ecol. Eng.,114, 34-45, doi:10.1016/j.ecoleng.2017.06.068, 2018.

780   Veldkamp, E., Koehler, B. and Corre, M. D.: Indications of nitrogen-limited methane uptake in tropical forest soils, Biogeosciences., 10, 5367–5379, doi:10.5194/bg-10-5367-2013, 2013.

Verchot, L. V., Dannenmann, M., Kengdo, S. K., Njine-Bememba, C. B., Rufino, M. C., Sonwa, D. J. and Tejedor, J.: Land-use change and Biogeochemical controls of soil CO_2, N_2O and CH_4 fluxes in Cameroonian forest landscapes, J. Integr. Environ. Sci., 00, 1–23, doi:10.1080/1943815X.2020.1779092, 2020.

785   Wang, C. K., and Yang J. Y.: Rhizospheric and heterotrophic components of soil respiration in six Chinese temperate forests. Glob. Chang. Biol., 13:123–131, doi.org/10.1111/j.1365-2486.2006.01291.x, 2007.

Wang, Z., Zhang, X., Liu, L., Cheng, M. and Xu, J.: Spatial and seasonal patterns of atmospheric nitrogen deposition in North China, Atmospheric Sci. Lett., 13(3), 188-194, doi.org/10.1080/16742834.2019.1701385, 2020.

Wanyama, I., Pelster, D. E., Butterbach-Bahl, K., Verchot, L. V., Martius, C. and Rufino, M. C.: Soil carbon dioxide

790   and methane fluxes from forests and other land use types in an African tropical montane region, Biogeochemistry., 143, 171–190, doi:10.1007/s10533-019-00555-8, 2019.

Wei, Z., Jiangming, M., Yunting, F., Xiankai, L. and Hui, W.: Effects of nitrogen deposition on the greenhouse gas fluxes from forest soils, Acta Ecol. Sin., 28(5), 2309–2319, doi:10.1016/S1872-2032(08)60047-5, 2008.

Wolf, K., Veldkamp, E., Homeier, J. and Martinson, G. O.: Nitrogen availability links forest productivity, soil nitrous

795   oxide and nitric oxide fluxes of a tropical montane forest in southern Ecuador, Global Biogeochem. Cycles., 25, doi:10.1029/2010GB003876, 2011.

Wright, S. J., Yavitt, J. B., Wurzburger, N., Turner, B. L., Tanner, E. V., Sayer, E. J., Santiago, L. S., Kaspari, M., Hedin, O, L., Harms, E, K., Garcia, N. M., and Corre, M. D.: Potassium, phosphorus, or nitrogen limit root allocation, tree growth, or litter production in a lowland tropical forest. Ecology., 92(8), 1616-1625, doi: 10.1890/10-1558.1, 2011.

800   Xu, H., Detto, M., Fang, S., Chazdon, R. L., Li, Y., Hau, B. C. H., Fischer, G. A., Weiblen, G. D., Hogan, J. A., Zimmerman, J. K., Uriarte, M., Thompson, J., Lian, J., Cao, K., Kenfack, D., Alonso, A., Bissiengou, P., Memiaghe, H. R., Valencia, R., Yap, S. L., Davies, S. J., Mi, X. and Yao, T. L.: Soil nitrogen concentration mediates the

relationship between leguminous trees and neighbor diversity in tropical forests, Commun. Biol., 3, 1–8, doi:10.1038/s42003-020-1041-y, 2020.

805 Yan, Y., Sha, L., Cao, M., Zheng, Z., Tang, J., Wang, Y., Zhang, Y., Wang, R., Liu, G., Wang, Y. and Sun, Y.: Fluxes of CH_4 and N_2O from soil under a tropical seasonal rain forest in Xishuangbanna, Southwest China, J. Environ. Sci., 20, 207–215, doi:10.1016/S1001-0742(08)60033-9, 2008.

Yu, L., Wang, Y., Zhang, X., Dörsch, P. and Mulder, J.: Phosphorus addition mitigates N_2O and CH_4 emissions in N-saturated subtropical forest, SW China, Biogeosciences., 14, 3097–3109, doi:10.5194/bg-14-3097-2017, 2017.

810 Zhang, T., Zhu, W., Mo, J., Liu, L. and Dong, S.: Increased phosphorus availability mitigates the inhibition of nitrogen deposition on CH_4 uptake in an old-growth tropical forest, southern China, Biogeosciences., 8, 2805–2813, doi:10.5194/bg-8-2805-2011, 2011.

Zhang, W., Mo, J., Yu, G., Fang, Y., Li, D., Lu, X. and Wang, H.: Emissions of nitrous oxide from three tropical forests in Southern China in response to simulated nitrogen deposition, Plant Soil., 306, 221–236, doi:10.1007/s11104-008-

815 9575-7, 2008.

Zhang, Y., Ma, M., Fang, H., Qin, D., Cheng, S. and Yuan, W.: Impacts of nitrogen addition on nitrous oxide emission : Comparison of five nitrous oxide modules or algorithms, Ecol. Modell., 421, 108963, doi:10.1016/j.ecolmodel.2020.108963, 2020.

Zheng, M., Zhang, T., Liu, L., Zhang, W., Lu, X. and Mo, J.: Effects of nitrogen and phosphorus additions on soil

820 methane uptake in disturbed forests, J. Geophys. Res., 121, 3089–3100, doi:10.1002/2016JG003476, 2016.

825

830

835

840

Supplementary figures
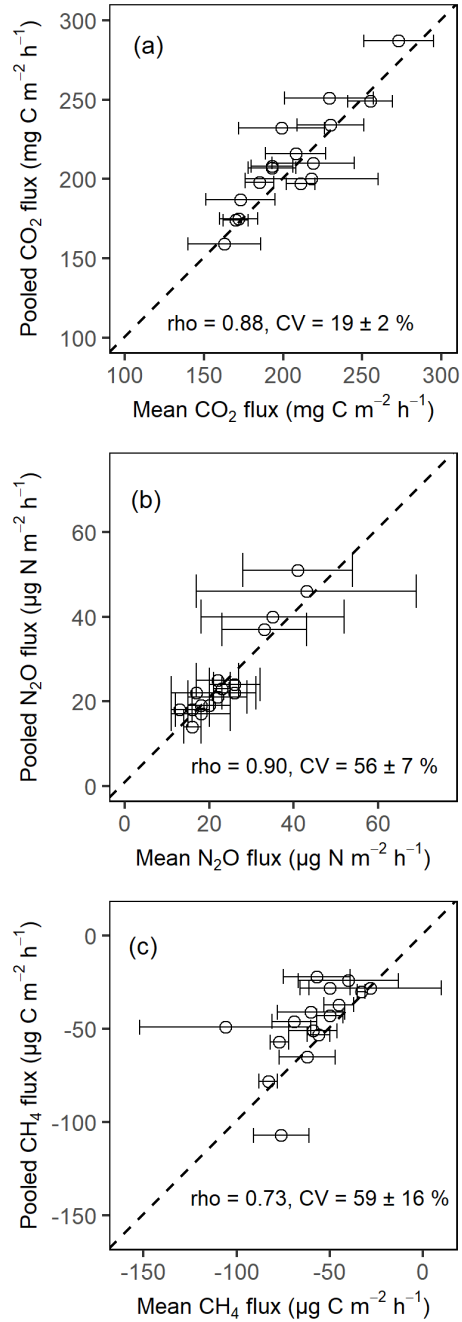
845   Supplementary figure 1. Comparison of the soil CO_2 fluxes (a) soil N_2O fluxes (b), and soil CH_4 fluxes (c) from pooled sampling and the mean of four chamber measurements for the month of February 2020 in Budongo Forest reserve. Rho is the spearman correlation coefficient, and CV is the coefficient of variation. Error bars are derived from standard error of the mean.